

# **High Throughput Screening of Gene Expression for the Investigation of Multifactorial Dermatological Disorders**

by

**Máté Manczinger MD.**

Supervisors:

Lajos Kemény MD, PhD, DSc and Lóránt Lakatos PhD

PhD Thesis

Department of Dermatology and Allergology  
University of Szeged, Hungary

2016

## **Publications directly related to the subject of the thesis**

- I. **Manczinger M**, Bocsik A, Kocsis GF, Voros A, Hegedus Z, et al. (2015) The Absence of N-Acetyl-D-glucosamine Causes Attenuation of Virulence of *Candida albicans* upon Interaction with Vaginal Epithelial Cells In Vitro. *Biomed Res Int* 2015: 398045. **IF: 1.579**
- II. **Manczinger M**, Kemeny L (2013) Novel factors in the pathogenesis of psoriasis and potential drug candidates are found with systems biology approach. *PLoS One* 8: e80751. **IF: 3.23**

## **Other publications**

- I. Guban B, Vas K, Balog Z, **Manczinger M**, Bebes A, et al. (2015) Abnormal regulation of fibronectin production by fibroblasts in psoriasis. *Br J Dermatol*. **IF: 4.225**
- II. Palotai M, Bagosi Z, Jaszberenyi M, Csabafi K, Dochnal R, **Manczinger M**, et al. (2013) Ghrelin and nicotine stimulate equally the dopamine release in the rat amygdala. *Neurochem Res* 38: 1989-1995. **IF: 2.551**
- III. Palotai M, Bagosi Z, Jaszberenyi M, Csabafi K, Dochnal R, **Manczinger M**, et al. (2013) Ghrelin amplifies the nicotine-induced dopamine release in the rat striatum. *Neurochem Int* 63: 239-243. **IF: 2.650**
- IV. Heinzlmann A, Kiss G, Toth ZE, Dochnal R, Pal A, Sipos I, **Manczinger M**, et al. (2012) Intranasal application of secretin, similarly to intracerebroventricular administration, influences the motor behavior of mice probably through specific receptors. *J Mol Neurosci* 48: 558-564. **IF: 2.891**
- V. **Manczinger M**, Szabo EZ, Goblos A, Kemeny L, Lakatos L (2012) Switching on RNA silencing suppressor activity by restoring argonaute binding to a viral protein. *J Virol* 86: 8324-8327. **IF: 5.076**
- VI. Koves K, Kiss G, Heinzlmann A, Dochnal R, **Manczinger M**, et al. (2011) Secretin attenuates the hereditary repetitive hyperactive movements in a mouse model. *J Mol Neurosci* 43: 109-114. **IF: 2.504**

## Table of contents

Publications directly related to the subject of the thesis .....	1
Other publications .....	1
Table of contents .....	2
List of abbreviations .....	4
1. Introduction .....	5
1.1. The role of systems biology in the research of multifactorial diseases .....	5
1.2. Vulvovaginal candidiasis.....	6
1.2.1. Epidemiology .....	6
1.2.2. Clinical characteristics .....	6
1.2.3. Pathogenesis and immune defense.....	6
1.3. Psoriasis .....	8
1.3.1. Epidemiology and clinical characteristics.....	8
1.3.2. Pathophysiology.....	8
1.3.3. Treatment .....	8
1.4. High throughput screening of gene expression .....	9
1.4.1. Microarray.....	9
1.4.2. Next generation sequencing .....	9
1.5. Network analysis .....	10
1.5.1. Introduction.....	10
1.5.2. Scale-free networks, centralities and motifs .....	10
1.5.3. Network analysis in biomedical research and drug development.....	11
2. Aims I.....	12
3. Aims II.....	12
4. Methods I.....	13
4.1. Strains, growth conditions and cell culturing .....	13
4.2. Viability test .....	13
4.3. <i>C. albicans</i> adherence assay.....	14
4.4. Total RNA isolation and high throughput sequencing .....	14
4.5. Bioinformatical and statistical analysis .....	15
4.6. Quantitative reverse transcriptase polymerase chain reaction (QRT-PCR) .....	15
5. Methods II .....	17
5.1. Microarray meta-analysis .....	17
5.2. Construction of protein-protein, protein-DNA and chemical-protein interaction networks.....	18

5.3. General network analysis, identification of central nodes and motif detection.....	18
6. Results I.....	21
6.1. Vaginal epithelial cell - <i>C. albicans</i> co-culture as a model of vulvovaginal infection ..	21
6.2. Primary analysis of transcriptome data .....	21
6.3. Validation of RNA-Seq data by quantitative real-time PCR (QRT-PCR) .....	23
6.4. Functional analysis of RNA-Seq data .....	24
6.4.1. Analysis of signal transduction pathways involved in hyphal morphogenesis.....	24
6.4.2. Expression analysis of genes involved in GlcNAc metabolism .....	26
6.4.3. Virulence of HXK1 mutant <i>Candida albicans</i> is decreased.....	27
6.4.4. GlcNAc is involved in the adherence of <i>C. albicans</i> to vaginal epithelial cells .....	29
7. Results II .....	31
7.1. Detection of DEGs with microarray meta-analysis.....	31
7.2. General Network analysis.....	32
7.3. Determination of hubs in DEG-derived networks.....	33
7.4. Motif analysis in DEG-derived networks.....	34
7.5. Controller sub-network construction .....	35
7.6. Analysis of chemical-protein interaction networks .....	38
7.7. Effective drugs predominantly act on proteins of the controller sub-network .....	42
8. Discussion .....	43
8.1. In vitro modelling vs. biopsy specimens .....	43
8.1.1. Vulvovaginal Candidiasis .....	43
8.1.2. Psoriasis .....	44
8.2. Filtering data and identification of important genes.....	44
8.2.1. Vulvovaginal candidiasis .....	44
8.2.2. Psoriasis .....	44
8.3. Putting genes in context.....	45
8.3.1. Vulvovaginal candidiasis .....	45
8.3.2. Psoriasis .....	46
8.4. Therapeutic aspects.....	48
8.5. The place of systems biology in dermatological research.....	49
Acknowledgement.....	50
References .....	51

## List of abbreviations

AE	acetate EDTA
APC	antigen presenting cell
ATC classification	anatomical therapeutic chemical classification
<i>C. albicans</i>	<i>Candida albicans</i>
cDNA	complementary desoxiribonucleic acid
CI	cell index
CKM	complete keratinocyte medium
control hyphae	<i>C. albicans</i> hyphae three hours post infection in serum free CKM without PK E6/E7 VECL cells
cph1 $\Delta$	cph1 mutant
dac1 $\Delta$	dac1 mutant
DEG	differentially expressed gene
EDTA	ethylenediaminetetraacetic acid
efg1 $\Delta$	efg1 mutant
ePCR	emulsion polymerase chain reaction
EtOH	ethanol
FDR	false discovery rate
GEO	Gene Expression Omnibus
GlcNAc	N-acetylglucosamine
HCl	hydrogen chloride
hgc1 $\Delta$	hgc1 mutant
hvk1 $\Delta$	hvk1 mutant
MHC	major histocompatibility complex
model hyphae	<i>C. albicans</i> hyphae three hours post infection in serum free CKM infected with PK E6/E7 VECL cells
mRNA	messenger ribonucleic acid
nag1 $\Delta$	nag1 mutant
NaOAc	sodium acetate
ngt1 $\Delta$	ngt1 mutant
nrg1 $\Delta$	nrg1 mutant
nt	nucleotide
PASI	psoriasis area and severity index
PCR	polymerase chain reaction
PDI	protein-DNA interaction
PPI	protein-protein interaction
QRT-PCR	quantitative real-time polymerase chain reaction
RIN	RNA integrity number
RNA-Seq	ribonucleic acid sequencing
RTCA	real time cell analysis
SD	standard deviation
SDS	sodium dodecyl sulfate
TBE	tris borate EDTA
TCR	T cell receptor
TE	tris EDTA
TF	transcription factor
Th1	T helper 1 cell
Th17	T helper 17 cell
VECL	vaginal epithelial cell line
VVC	vulvovaginal candidiasis
YPD	1% yeast extract, 2% peptone, 2% glucose/dextrose

# 1. Introduction

## *1.1. The role of systems biology in the research of multifactorial diseases*

Most common diseases are caused by numerous internal and environmental factors. Multiple intracellular discrepancies in gene expression and in protein abundance can be found causing the phenotype of these diseases. Thus, the investigation of the system instead of one gene or protein have become necessary to understand disease mechanisms and find the most effective treatments [1]. I am going to demonstrate high-throughput gene expression studies for two multifactorial diseases: the infectious vulvovaginal candidiasis (VVC) and the non-infectious psoriasis. In the first study, we constructed an in vitro model of VVC and carried out RNA-Seq analysis to identify virulence factors of the fungus. In the second one, we have done a meta-analysis of published microarray data about psoriasis, which was further processed in silico with a network-based approach. In both studies, we looked for potential proteins, which may have role in pathogenesis and could be modulated with drugs. We identified potential drug candidates as well for psoriasis.

The physiologic and pathogenic role of the microbiome has become an important field of medical sciences in the recent years. Huge amount of large-scale data about microorganisms in the normal human flora is available in multiple databases. Genetic, genomic, metagenomic, epigenomic, transcriptomic, proteomic, metabolomic and evolutionary analysis have become main-stream methods in biomedical research [2]. High throughput sequencing made it possible to analyze genomes, epigenomes, transcriptomes and the constitution of microbes during infection. As a result, more effective identification of virulence factors and, thus, potential drug targets have become possible [3].

Psoriasis is one of the most studied skin diseases. More than 39000 hits are available currently in PubMed for the keyword „psoriasis” and the number is increasing. “Omics” data gives the opportunity to examine the disease with systems biology approach. With this, it has become possible to reveal new treatment options and to understand the disease better [4]. The way we handle huge datasets is crucial to get reliable results. The proper use of bioinformatics tools for filtering, normalization and statistical processing is essential to avoid false inferences. In silico model construction is possible only after these steps [5].

## **1.2. Vulvovaginal candidiasis**

### *1.2.1. Epidemiology*

Infections related to candida species are common. The majority of infections are caused by *C. albicans*, although the prevalence of other, non-*albicans* Candida species is increasing [6,7]. Candidiasis affects the mucosal surfaces and the skin of healthy people, but life-threatening invasive candidiasis can be developed in severely immunocompromised individuals [7]. *C. albicans* is the member of the normal vaginal flora in 10-20 % of women and can be found in the normal oral flora of individuals ranging from 7.7 to 70% depending on geographical factors [8]. Most common form of *C. albicans* infections is VVC. 75 % of women are affected at least once in their lives, and around 5 - 10% of them have recurrent infections [6]. Prevalence of the disease is affected by sexual activity, age, diabetes mellitus, the use of antibiotics, pregnancy etc. [9]

### *1.2.2. Clinical characteristics*

VVC frequently affects otherwise healthy women. However, the disease is more common in patients with diabetes mellitus, after the use of broad-spectrum antibiotics and during pregnancy [9]. Interestingly, the prevalence is not increased in diseases, which are characterized with decreased adaptive immune defense [6]. Most important signs of VVC are the erythema, the itch of the vulva, the erythema of the vagina, and a thick, white discharge [10].

### *1.2.3. Pathogenesis and immune defense*

*C. albicans* is a dimorphic fungus exhibiting non-pathogenic yeast morphology as a member of the normal human flora as well as pathogenic hyphal morphology. *C. albicans* is adapted to its mammalian host in several ways and hyphal growth can be induced by several factors. Everything that makes the environment unfavorable for the fungus, induces the hyphal transcriptional program [11]. Filamentous form causes cell damage by penetration. Induced phagocytosis of the yeast is also prevalent. Several invasin molecules mediate the uptake of the fungus by host cells [12]. Filamentous growth is then initiated in the phagosome and hyphae cause cell lysis [13].

Morphological switch itself is required for pathogenesis as virulence is decreased in mutants constantly staying in yeast (*efg1Δ/cph1Δ*, *hgc1Δ*) or hyphal (*nrg1Δ*) morphologies. A complicated signal transduction network regulates this switch [11]. The dimorphism has an

effect on the antigenicity, thus, immune evasion of *C. albicans* [12]. An important initial step during pathogenesis is adhesion. A large set of adhesins and a complex regulatory machinery have already been identified [14]. After adhesion and hyphal induction, penetration is facilitated by a set of secreted aspartic proteases [15]. Several fitness traits can also be considered as virulence factors, such as the stress response by heat shock proteins, auto-induction of filamentation, metabolic flexibility and the uptake of metals and other compounds [12].

Differentiation between the two forms is present on the level of innate recognition. Pattern recognition receptors recognize glycoproteins on the surface of the fungus in a non-specific way. The cell wall constitution of yeast is different from hyphae [16]. Cell wall remodeling starts at the beginning of filamentation. Filamentous form induces immune-response, while the commensal form is less immunogenic [16].

The particular role of adaptive immunity against *C. albicans* is less well described. Several studies reported the presence of *C. albicans*-specific antibodies in the circulation [17,18]. Induction of the cellular adaptive immune response, which has also been described, contributes more significantly to defense mechanisms against candidal infection, than humoral factors. Cellular adaptive immune response against *C. albicans* (and numerous other fungal pathogens) involves antigen presenting cells (APCs), such as macrophages and dendritic cells, which present short peptides (epitopes) bound to major histocompatibility complex (MHC) II molecules on the cell surface. *C. albicans*-specific epitopes are recognized by T-cell receptors (TCRs) on the surface of T helper (Th) cells [19]. Taking place at the so-called immunological synapse, immunological recognition involves APCs, MHC II molecules, epitopes, TCRs and Th cells [20]. Epitope binding to its specific TCR activates Th1 and Th17 cells, which then recruit neutrophil granulocytes and monocytes to the place of infection by expressing interferon gamma or IL17 [19,21]. Noteworthy, that the site of infection significantly affect immune response. While adaptive immune system has a significant role during the course of the disease on the mucosal surfaces of the gastrointestinal tract, only the role of innate immunity is supposed in case of VVC [6].



### **1.3. Psoriasis**

#### *1.3.1. Epidemiology and clinical characteristics*

Psoriasis is a multifactorial inflammatory skin disease. A recent systematic review reported a prevalence from 0% (Taiwan) to 2.1% (Italy) in children and from 0.91% (United States) to 8.5% (Norway) in adults [22]. Psoriasis is more common in the Caucasian race compared to African Americans in the USA [23]. The disease is usually chronic and recurrent. Patients have hyperkeratotic, scaly patches on their skin. Predilection sites are the elbows, knees and the sacral area, but it can also affect the scalp, nails and the whole skin surface [24]. Sometimes very severe forms can be developed affecting almost 100% of the skin. This life-threatening condition is called erythroderma. Psoriasis is associated with a rheumatic disease called psoriatic arthritis, which develops in 5 - 30% of psoriasis patients [24].

#### *1.3.2. Pathophysiology*

Genetic predisposition and environmental factors are both important in disease etiology. Several genome-wide association studies have been carried out and until now 36 susceptibility loci have been identified [25]. Environmental triggers are also reported such as drugs, smoking, mental stress, skin injury, Streptococcal infection, hormonal changes etc [26]. Psoriasis is an immune-mediated disease. Important immune cells and cytokines have been identified in disease pathogenesis such as IL6, IL17A, TNF etc [27]. Autoimmune basis for chronic inflammation is supposed, although no consistent antigen has been found. Patients with psoriasis have higher risk for metabolic syndrome, and risk increases with disease severity. Both diseases have immunological basis with common cytokines and genetic risk loci like CDKAL1 [28]. Keratinocyte hyperproliferation is present in lesional phenotype and is responsible for scale formation. Keratinocyte differentiation markers like keratin 1 and keratin 10 are downregulated and parakeratosis (keratinocytes with nuclei in the stratum granulosum) is present [26].

#### *1.3.3. Treatment*

Numerous treatment options are available, but no “golden standard” have been developed. Treatment recommendations vary depending on disease severity, co-morbidities and treatment history [24]. Treatment options can be classified into local, UV-light and systemic groups. Most common local therapies are steroids, vitamin D3 analogues, dithranol, retinoids and calcineurin inhibitors. Mainstream systemic therapeutic options are methotrexate, calcineurin inhibitors and biological therapy [24].

A general consideration is that different patients respond to treatment options with different extent. In some cases, treatment worsens the disease instead of improving it. There are also treatment-resistant cases [29]. All of these facts suggest, that psoriasis is much more complex than how we are now understanding it and systematic analysis of the diseases is required to acquire further aspects of pathogenesis.

#### ***1.4. High throughput screening of gene expression***

##### *1.4.1. Microarray*

Stationary changes in gene expression are responsible for fixing phenotypes such as the lesional skin area in psoriasis. DNA microarray is a widely used method for large-scale screening of gene expression. Fixed DNA probes binding different DNA sequences are fixed to a solid surface. RNA is reverse transcribed to DNA and then complementary DNA (cDNA) is fluorescently labelled. cDNA is then hybridized to DNA on the microarray chip, and the non-specific sequences are washed down. Laser-based detection of the fluorescence is possible, which is proportional with the abundance of sequence specific cDNA, thus with the abundance of mRNA [30]. Large scale screening of splicing, single nucleotide polymorphisms (SNP), transcription factor binding sites, fusion genes etc. has become possible with the improvement of microarray technology. After registering fluorescence, in silico normalization and filtering of data is crucial [5]. Microarray is relatively cheap and broad spectrum of bioinformatical methods and libraries are present for the analysis of microarray data [5]. One disadvantage opposed to high-throughput sequencing is, that microarray cannot reveal new transcripts, only predestinated sequences can be detected [31].

Several microarray studies have been carried out to characterize gene expression in healthy and psoriatic skin samples (Table 1). Microarray meta-analysis gives the opportunity to evade biological, regional, and study design-caused variation between studies [32].

##### *1.4.2. Next generation sequencing*

High throughput sequencing technologies emerged in the 1990s [33]. Researchers are able to get sequences of whole genomes and transcriptomes, but these technologies can also be used for different other purposes like characterizing DNA-protein interactions (ChIP-sequencing) and the epigenome. The cost of these assays were high, but the price is constantly getting lower making their use possible in basic research [34]. Compared to the classical “chain termination” based Sanger sequencing, these methods are much faster, have higher sequencing capacity and lower cost. The most popular ones are ligation based sequencing (SOLiD),

synthesis-based sequencing (Illumina), pyrosequencing (454) and ion torrent sequencing methods [34].

We used SOLiD sequencing for our VVC study. A large set of possible polynucleotide sequences with fixed length is labelled and ligated to the query DNA sequence. This ligation results in signal, which is detected by the sequencer. It is important to amplify the cDNA by emulsion PCR before ligation [35].

Beside the already mentioned advantages of next generation sequencing, another one is its ability to identify novel transcripts. Although the cost of these methods is getting lower, it can be still very expensive to use biological replicates. If this is the case, validation of results is essential.

## ***1.5. Network analysis***

### *1.5.1. Introduction*

Network analysis is a novel and highly developing area of systems biology. Considering gene expression data, it is possible to explain alterations in intracellular processes with the analysis of protein-protein and protein-DNA (or gene regulatory) interaction networks. These networks consist of proteins and/or regulated genes as nodes and undirected or directed edges between them [36].

### *1.5.2. Scale-free networks, centralities and motifs*

Centralities, like degree or stress, are suitable for ranking nodes. Total edge number belonging to one node equals its degree in undirected networks. Nodes have in- and out-degrees based on edge directions in directed networks [36]. Degree values follow a scale-free power law distribution in biological networks. This fact indicates that highly connected vertices have a large chance of occurring. Nodes with highest degree are called hubs and are essential in network stability [37]. Stress centrality indicates the number of shortest paths (from all shortest paths between any two nodes in the network) passing through the given node and, thus, the capability of a protein to hold together communicating nodes [38]. Interconnected nodes make up network motifs. Several motifs, such as the feed-forward or bifan motif are significantly enriched in biological networks compared to random networks. These elements have important role in network dynamics [39].

### *1.5.3. Network analysis in biomedical research and drug development*

It is important to investigate intracellular proteins as members of an intracellular network. Since the description of scale-free networks in the late 90s, rapid development can be seen in the field of network-based analysis of large-scale datasets [40]. Multiple *in silico* methods and software are developed and are widely used. We can consider biological pathways as networks and analyze processes instead of individual proteins, genes or metabolites. A large set of pathway databases is available online like KEGG, Reactome, Ingenuity etc. [41] We can also construct custom networks based on protein-protein and protein-DNA interaction databases, like STRING or CisRED [42,43].

Network analysis is also prevailing in drug discovery. Identification of new drug targets is essential. For this, first, the integration of all information about the model biological system is needed. The most plausible way is to create networks. Network based approaches can help us to predict drug side-effects, drug-drug interactions and can be used in numerous other fields of drug discovery [4].

## **2. Aims I**

Despite recent advances are made in our understanding of disease pathogenesis caused by *C. albicans*, little is known about the mechanisms that underlie hyphal transition in response to contact with human vaginal epithelial cells. We managed to construct an in vitro model of VVC. We hypothesized that the characteristics of hyphae growing in the presence of human cells is markedly different from control hyphae, which grow without human cells. We also supposed, that genes, that are solely differentially expressed in the presence of human cells can potentially be virulence factors.

## **3. Aims II**

Our goal was to construct reliable but yet detailed protein-protein, protein-DNA, merged (containing both protein-protein and protein-DNA interactions) and chemical-protein interaction networks consisting of differentially expressed genes (DEG) between lesional and non-lesional skin samples of psoriatic patients and/or the coded proteins. We hypothesized, that it could be possible to find novel elements in psoriasis pathogenesis and potential drug candidates with the detailed analysis of these networks.

## 4. Methods I

### 4.1. Strains, growth conditions and cell culturing

*C. albicans* clinical isolate SC5314 was grown on YPD medium at 30°C, cultured under standard conditions until logarithmic phase, and then counted with a haemocytometer. The immortalized human vaginal epithelial cell line (VECL) PK E6/E7 [44] was cultured in serum-free complete keratinocyte medium (CKM) supplemented with 5 ng/mL recombinant epidermal growth factor, 50 µg/mL bovine pituitary extract, L-glutamine, and antibiotic/antimycotic solution (all from Life Technologies) in a CO<sub>2</sub> thermostat at 37°C [45]. Cells at 60–70% confluency were used in subsequent experiments. A total of 10<sup>5</sup> PK E6/E7 VECL cells were seeded in 6-well plates and incubated for 24 hours in serum-free CKM. At 24 hours prior to infection with *C. albicans*, the medium was changed to serum-free CKM (pH 8.0) without antibiotic/antimycotic solution. Fungal cells were collected in log phase, washed three times with CKM, and then resuspended in complete CKM without antibiotic/antimycotic solution to eliminate farnesol. In order to induce hyphal growth, plates were incubated in a CO<sub>2</sub> thermostat at 37°C (control hyphae). Fungal cells, treated the same way, were added to wells with a multiplicity of infection (MOI) of 3:1 to infect PK E6/E7 VECL cells. Yeast control cells were harvested at 0 hour time point. Plates were incubated for 3 hours in a humidified atmosphere containing 5% CO<sub>2</sub> at 37°C; fungal cells rapidly switch to filamentous growth under such circumstances. Ten randomly chosen fields of view were used to count *C. albicans* hyphae penetrating into vaginal epithelial cells.

### 4.2. Viability test

The effect of *C. albicans* infection on the viability of PK E6/E7 VECL cells was measured by Real-Time Cell Analysis (RTCA; ACEA Biosciences), as described previously [46-48]. Briefly, 10<sup>4</sup> PK E6/E7 cells per well were seeded in 96-well E-plates (ACEA Biosciences) in which the bottom of the wells were covered with micro electrodes. Epithelial cells were allowed to attach to the bottom of the wells and grow for 3 days. Cells were then treated with 2 × 10<sup>3</sup>, 5 × 10<sup>3</sup>, 1 × 10<sup>4</sup>, and 2 × 10<sup>4</sup> *C. albicans* h<sub>xk1</sub>Δ or DIC185 cells/well. Triton-X (Sigma) treatment was used as a positive control to kill the vaginal epithelial cells. Real-time measurements of impedance were done with the xCELLigence System RTCA HT Instrument (ACEA Biosciences); the impedance was monitored every 10 minutes. The cell index at each time point was defined as  $(R_n - R_b)/15$ , where  $R_n$  is the cell-electrode impedance of the well when it contains cells and  $R_b$  is the background impedance of the well

with the medium alone. The cell index (CI) was normalized to the latest time point before the treatment of each group (CI<sub>n</sub>/CI before treatment) or presented as percent of non-treated control group [(CI<sub>n</sub>/CI average of control group) × 100]. CI values reflect cell number, adherence, cell growth, and health. Data is presented as means ± standard deviation (SD). Statistical significance between treatment groups was determined using one-way and two-way ANOVA following pairwise T tests with Bonferroni correction (GraphPad Prism 5.0; GraphPad Software). Experiments were repeated three times and the number of biological replicates varied between 3 and 6.

### **4.3. *C. albicans* adherence assay**

PK E6/E7 VECL cells were grown in 6-well plates until confluency was reached (>90%). The *hck1Δ* mutant and the parental strain (DIC185) [49] were grown on YPD plates for 24 hours. A total of 10<sup>5</sup> cells re-suspended in CKM were used to infect vaginal epithelial cells for 90 minutes. Supernatant was then aspirated and the wells were washed two times with 1× PBS. The monolayers with attached *C. albicans* were fixed by 3.7% (v/v) paraformaldehyde in PBS. Quantitation of *C. albicans* adherence was performed by light microscopy at a 25x magnification. Ten randomly chosen fields of view covered with epithelial cells were counted. Significance was calculated with a two-sample T test and a p value of less than 0.05 was considered to be significant. Experiments were performed with three biological replicates.

### **4.4. Total RNA isolation and high throughput sequencing**

Cells were harvested and re-suspended in 400 μL AE buffer (50 mM NaOAc, 10 mM EDTA); 40 μL 10% SDS and 440 μL of phenol were added and the samples were vortexed. The mix was incubated at 65°C for 10 minutes and frozen in liquid nitrogen. After thawing, the samples were centrifuged with 10000 G for 2 minutes; the upper phase was extracted with phenol-chloroform and precipitated with 1/10th volume of 3 M NaOAc and 2.5 × volume of 96% ice cold EtOH. Finally, the samples were centrifuged (10000 G, 15 min), the supernatant was discarded, and the pellet was washed with 70% EtOH and resuspended in TE buffer (10 mM Tris-HCl, 1 mM EDTA, pH 7.5). RNA quality and quantity measurements were performed on Bioanalyzer (Agilent Technologies) and Qubit (Life Technologies). Whole transcriptome sequencing was performed as described previously [50]. Briefly, total RNA samples from three biological replicates were pooled in equimolar concentrations and processed using the SOLiD total RNA-Seq Kit (Life Technologies), according to the manufacturer's instructions. For this, 5 μg of pooled RNA was DNaseI treated and fragmented using RNaseIII;

the eukaryotic ribosomal RNA was depleted prior to fragmentation using RiboMinus Eukaryote Kit for RNA-Seq and RiboMinus Concentration Module (Life Technologies). Next, the 50–200 nt RNA fraction was size-selected, sequencing adaptors were ligated, and the templates were reverse-transcribed using ArrayScript reverse transcriptase. The cDNA library was purified with Qiagen MinElute PCR Purification Kit (Qiagen) and size-selected on a 6% TBE-Urea denaturing polyacrylamide gel. The 150–250 nt cDNA fraction was amplified using AmpliTaq polymerase and purified by AmPureXP Beads (Agencourt). The concentration of each library was determined using the SOLiD Library TaqMan Quantitation Kit (Life Technologies). Each library was clonally amplified on SOLiD P1 DNA Beads by emulsion PCR (ePCR). Emulsions were broken with butanol and ePCR beads were enriched for template-positive beads by hybridization with magnetic enrichment beads. Template-enriched beads were extended at the 3' end in the presence of terminal transferase and 3' bead linker. Beads with the clonally amplified DNA were deposited onto SOLiD flowchip and sequenced on SOLiD V4 instrument using the 50 + 35-base paired-end sequencing chemistry.

#### ***4.5. Bioinformatical and statistical analysis***

Bioinformatical analysis of the whole transcriptome sequencing was performed in color space using Genomics Workbench (CLC Bio). Raw sequencing data was trimmed by removal of low quality, short sequences so that only 50 + 35 nucleotide long sequences were used in further analysis. Sequences were mapped in a strand specific way onto the *C. albicans* SC5314 assembly 19 reference genome [51] using default parameters except for the following: minimum length 50% and minimum similarity 80% with the unspecific match limit set to 10. Normalized gene expression was calculated using the “scaling” normalization method [52]. The three sequenced libraries were deposited in NCBI’s Gene Expression Omnibus (GEO) Archive at [http://www.ncbi.nlm.nih.gov/geo/under accession GSE54694](http://www.ncbi.nlm.nih.gov/geo/under%20accession%20GSE54694). Differentially expressed genes from the RNA-Seq output were determined using the R package DEGSeq. The software calculates significance with an MA-plot method for RNA-Seq data without biological replicates. Gene expression was considered significantly different between two conditions if the false discovery rate (FDR) corrected probability (p) value was less than 0.05 [53] and the absolute fold change value was more than 2 [54].

#### ***4.6. Quantitative reverse transcriptase polymerase chain reaction (QRT-PCR)***

cDNA was synthesized from at least 100 ng of high quality (RIN > 8.5) total RNA by using the High Capacity RNA-to-cDNA Kit (Life Technologies) according to the



manufacturer's instructions. SybrGreen technology-based real-time quantitative PCR was used to quantify the relative abundance of the selected mRNAs. As controls, we used reaction mixtures without cDNA. Relative expression of the given gene in the yeast-like form was set to 1 and the expression in control hyphae and hyphae developed in the presence of PK E6/E7 vaginal epithelial cells was calculated by comparing the values to the yeast form. Two technical and three biological replicates were used. The ratio of each mRNA relative to the 18S rRNA was calculated using the  $2^{-\Delta\Delta CT}$  method; all the data are presented as mean  $\pm$  SD. Differential expression was assessed with one-way ANOVA followed by pairwise t-test and Bonferroni p value correction.

## 5. Methods II

### 5.1. *Microarray meta-analysis*

Six microarray studies examining lesional and non-lesional skin biopsy samples of psoriatic patients were found in GEO (Table 1). “Minimum Information About a Microarray Experiment” (MIAME) was available for each study. Only non-lesional and lesional samples from affected individuals were used for analysis, samples of healthy individuals were excluded. Raw .CEL files were downloaded and quality of each sample was assessed with the R package *arrayQualityMetrics* [55]. This package defines sample quality with 5 different methods and generates plots for outlier detection. A sample was excluded if it was obviously an outlier in at least 1 measure or had borderline values in at least 2 measures. Raw data normalization of remaining samples was carried out with the R package *Easy Microarray data Analysis (EMA)*. [5] GCRMA normalization method was used and probe sets with expression level below 3.5 were discarded. Probe set with the highest interquartile range (IQR) was chosen for common HUGO Gene Nomenclature Committee (HGNC) gene identifiers. Original findings were confirmed with published statistics and EMA was used for this after GCRMA normalization. More DEGs were found in some cases, which might be caused by the pre-filtering process with *arrayQualityMetrics*. The R package *MetaQC* was used for filtering out low quality studies [56]. The fifty most prevalent gene sets were chosen with the software *Gene Set Enrichment Analysis (GSEA)* and used for external quality control (EQC) score calculation [57]. GSEA was carried out for each study with the following settings: 1000 permutations; minimum set size was 5 and the gene set database was *c2.all.4.0.symbols*. The resultant study-level p values of a gene set were combined with Fisher’s combined probability test. The fifty gene sets with the lowest meta-analysis p value were chosen as input for EQC score calculation. *C2.all.4.0.symbols* gene set database was chosen as input for consistency quality control (CQCp) value calculation. GSEA input expression matrices contained gene IDs that were present in all studies after EMA filtering. *MetaDE* package was used to determine DEGs in lesional samples compared to non-lesional ones [58]. DEG p values for individual studies was calculated by two sample T test with unequal variances. Fisher’s combined probability test was chosen for meta-analysis statistical method [59]. Fold change of gene expression was given by the ratio of gene expression geometrical means in lesional and non-lesional samples [60]. Genes with FDR less than 0.001 and with fold change higher than 1.5 or less than -1.5 were accepted as DEGs.

## ***5.2. Construction of protein-protein, protein-DNA and chemical-protein interaction networks***

STRING database 9.0 was used as resource for protein-protein interactions (PPI) [42]. Both directed and undirected networks were created by selecting all interactions between DEG – coded proteins in raw STRING data. Interactions with a confidence score higher, than 900 (“highest confidence” group) were used in case of undirected network construction and 800 (containing a part of “high confidence” and all “highest confidence” interactions) in case of directed network construction. Only directed interactions with “activation”, “inhibition” or “ptmod” action properties were used. Chemical-protein interactions between potential drugs, intra- and extracellular compounds and DEG-coded proteins were collected from STITCH database 3.1.[61] Confidence score calculation is the same in this database as in STRING thus interactions with the described confidence score cutoff values were selected for network construction. Protein-DNA interaction (PDI) network consisting of DEGs and DEG-coded transcription factors (TF) was created using cis-Regulatory Element Database (CisRED) [43]. Regulatory element motifs with  $p < 0.001$  were collected from DEG promoter regions. Motifs were coupled with TFs or TF complexes using TRANSFAC and JASPAR databases [62,63]. Motifs without respective TFs were excluded. Merged DEG-derived network containing PPI and PDI interactions and a network containing only DEG-coded TFs were also generated. Complete PPI, PDI, merged, TF-TF and chemical-protein interaction networks were created for controls using all available interactions in databases with the same statistical threshold as in DEG-derived network construction.

## ***5.3. General network analysis, identification of central nodes and motif detection***

General network analysis and node centrality value calculation were carried out with NetworkAnalyzer Cytoscape plugin [64]. Isolated nodes and node groups (without connection with the main PPI network) were deleted from graph in order to evade false results. Curve fitting on node degree and stress value distributions was done with MATLAB Curve Fitting Tool (MATLAB R2012b, The Mathworks Inc., Natick, MA). Curve of power law distribution was assessed with Trust-Region algorithm. Goodness of fit was assessed by R-square and corrected R-square values. Power law distribution of these node centralities was proven, as R-squared values were ranged from 0.87 to 1.0. As power law distribution is asymmetric with a long tail, it cannot be described with classical statistics used for Gaussian distribution. A variable with a power-law distribution has a probability  $P(k)$  of taking a value  $k$  following the

function  $P(k) \sim Ck^{-\gamma}$ , where  $C$  is constant. First moment (mean value) of a power-law distributed quantity equals:

$$\langle k \rangle = \frac{\gamma - 1}{\gamma - 2} k_{min}; (\gamma > 2)$$

Second moment (variance) of a power-law distributed quantity equals:

$$\langle k^2 \rangle = \frac{\gamma - 1}{\gamma - 3} k_{min}^2; (\gamma > 3)$$

The sum of first and second moment (mean value and variance) was used as cutoff for centralities with distribution exponent of  $\gamma > 3$ . Expression of variance becomes infinite, if  $\gamma \leq 3$ , thus only first moment (mean value) was used as cutoff for centralities with distribution exponent  $2 < \gamma < 3$  [65]. Expression of mean value becomes infinite, if  $\gamma \leq 2$ . In this case weighted mean was used to assess cutoff with the following formula:

$$\langle k \rangle = \frac{\sum_{i=0}^n k_i \frac{1}{C k_i^{-\gamma}}}{\sum_{i=0}^n \frac{1}{C k_i^{-\gamma}}}$$

As bidirectional connections are available in undirected PPI network, stress centrality is independent from edge directions, thus, both degree and stress had to be above cutoff for central protein selection. As directed networks contain unidirectional interactions, low stress values (i. e. low number of shortest paths cross through the node) can be caused by the dominance of incoming (in-degree) or outgoing (out-degree) interactions. Important nodes with high in-degree or out-degree can still have low stress centrality thus either out-degree or in-degree or stress had to be above cutoff in directed PPI network. As TFs have mainly outgoing interactions, out-degree was used for TF prioritization. Similarly to PPI networks, degree and stress had to be above cutoff in undirected chemical - protein interaction network. Drugs with more targets in DEG-derived PPI-networks may have bigger disease modifying effect, thus out-degree had to be above cutoff in directed chemical – protein interaction network for drug prioritization.

NetMODE software was used for network motif statistical analysis. Frequency of 3 or 4 node motifs in DEG-derived and complete control networks were compared with 1000 random graphs. *Local constant switching mode* was used for edge switching method during random network generation. NetMODE  $p$  value indicates the number of random networks in which a motif occurred more often than in the input network, divided by total number of random

networks.  $p < 0.05$  was used as cutoff [66]. Respective sub-networks of enriched motifs were identified with NetMatch Cytoscape plugin [67].

## 6. Results I

### 6.1. Vaginal epithelial cell - *C. albicans* co-culture as a model of vulvovaginal infection

Infection of epithelial cells by *C. albicans* requires adhesion of yeast form cells to the surface of epithelium. We used the immortalized PK E6/E7 VECL [44] cultured in serum-free CKM, containing 1.0 g/L (0.1 v/w%, or 5.6 mM) glucose, and infected them with *C. albicans* SC5314 yeast form cells (Figure 1a). Since we aimed to monitor the primary effect of human cells on hyphae formation, we sampled the cells at 3 hours post infection. Notably, conditions changed drastically in our culturing environment. CO<sub>2</sub> concentration and temperature increased, and neutral pH changed to alkaline, all of which are known to strongly induce the morphological transition of *C. albicans* [68]. Thus, *C. albicans* cells adhered to the surface of PK E6/E7 VECL and developed hyphae and approximately 5% of hyphae penetrated into epithelial cells (Figures 1c and 1d). We call this sample “model hyphae” for simplification.

*C. albicans* cells were cultured in serum-free CKM without human cells for 3 hours as control. Microscopic examination showed that at this time point *C. albicans* cells are adhering to the surface of the culture chamber and develop hyphae even in the absence of serum (Figure 1b). We call this sample “control hyphae” for simplification. Importantly, control hyphae and model hyphae could not be distinguished in terms of the timing of the morphological switch, rate of hyphae development, or length of hyphae (Figures 1b and 1c).

### 6.2. Primary analysis of transcriptome data

To study the early and specific molecular events occurring upon hyphae formation in the absence or presence of vaginal epithelial cells, global transcriptional changes of *C. albicans* cells were monitored using RNA-Seq. To do this, transcriptomes of yeast form *C. albicans*, control hyphae and model hyphae were sequenced on SOLiD System. Reads were aligned to the *C. albicans* SC5314 genome (assembly 19) and normalized gene expression values were calculated as described in materials and methods. Identification of DEGs between different forms of *C. albicans* was carried out with the R library DEGSeq. Genes with 2-fold absolute difference of gene expression and a FDR less than 0.05 were considered to be DEGs.

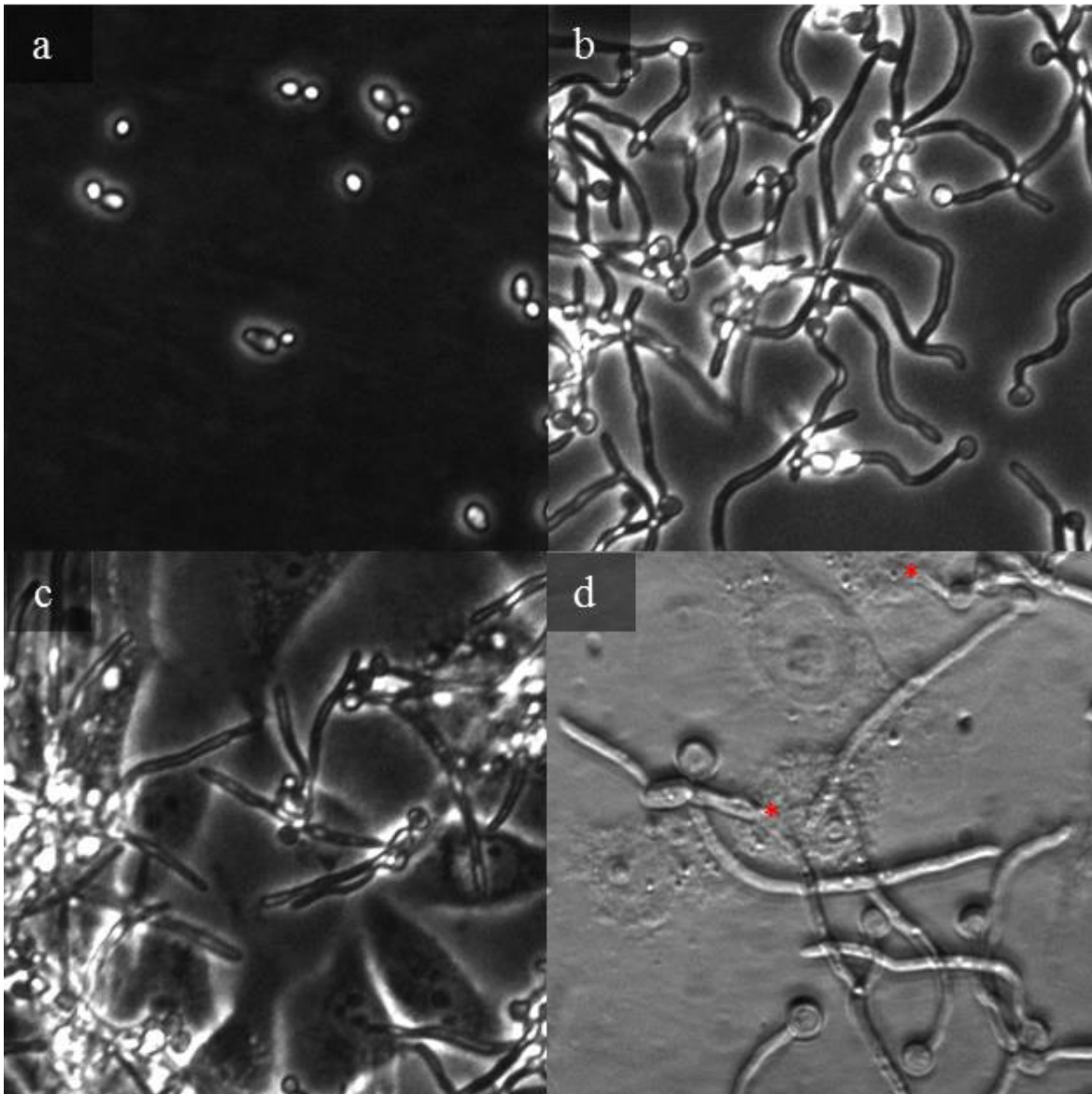


**Figure 1** Microscopic analysis of *C. albicans* hyphal growth in vitro. Yeast form of *C. albicans* (a); *C. albicans* develops hyphae in CKM (b) and in the presence of PK E6/E7 vaginal epithelial cells (c). *C. albicans* hyphae penetrate into PK E6/E7 VECL cells (d, penetration sites are marked with red asterisk).

Pairwise comparison resulted in 1283 DEGs between control hyphae and yeast. Surprisingly, almost twice as much, 2537 DEGs were found between model hyphae and yeast. We identified 1574 DEGs between the two hyphal forms. RNA-Seq data allowed us to identify 384 DEGs with higher expression in both hyphae compared to yeast and no difference between the two hyphal forms. These genes might be considered as effector genes of hyphae formation as a response of culturing *C. albicans* in serum-free CKM. We found 376 DEGs upregulated in both hyphal forms compared to yeast and differentially expressed between control and model

hyphae. 1205 DEGs were exclusively found between model hyphae and yeast. These genes may play an important role in the virulence of *C. albicans* after contact with vaginal epithelial cells.

### 6.3. Validation of RNA-Seq data by quantitative real-time PCR (QRT-PCR)

QRT-PCR analysis were performed to validate the expression pattern of 22 genes (Figure 2). This gene set includes representatives of all the identified expression patterns (see above). The QRT-PCR analysis showed, that 15 genes (among others, CHS8, HOG1, and CDC53) were indeed significantly upregulated in model hyphae, but not in control hyphae. ARX1, MUP1, and GDA1 were upregulated in both hyphal forms, but no significant difference was found between the two hyphae. GCN4, EAP1, and TES2 were upregulated in both hyphae and there was significantly higher expression in model hyphae compared to control hyphae. Finally, expression of FOX2 was significantly downregulated in both model and control hyphae. The results of QRT-PCR analysis are in complete agreement with the RNA-Seq expression data (Figure 2).

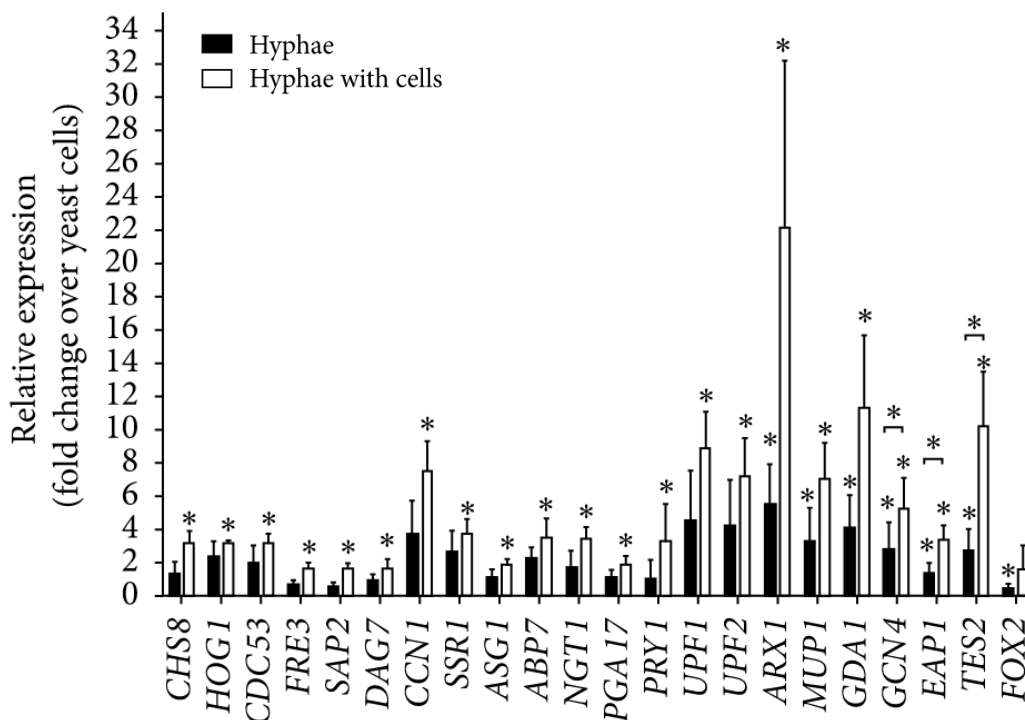


**Figure 2** QRT-PCR validation of RNA-Seq results. The relative gene expression of selected genes shows altered expression upon hyphae development as compared to yeast-like growth. Black and open bars represent control and model hyphae, respectively. Data are representative of 3 or more independent experiments and are presented as mean  $\pm$  SD. \* $p < 0.05$ .



## 6.4. Functional analysis of RNA-Seq data

### 6.4.1. Analysis of signal transduction pathways involved in hyphal morphogenesis

Our culturing conditions induced strong hyphal morphogenesis of *C. albicans* with or without PK E6/E7 VECL (Figure 1). We sought to determine if different signal transduction pathways leading to hyphal morphogenesis are responding to these conditions at the level of transcription. We found that the DCK1-RAC1 pathway, known to be required for filamentous growth in a matrix embedded microenvironment, is upregulated in control hyphae and further upregulated in model hyphae (Figure 3). Moreover, expression of MEP2 transducing low nitrogen signal towards RAS1 was also enhanced during hyphal growth (Figure 3). Neither the expression of the RAS1, which is known as a signal integrator, nor the expressions of CDC24 or STE11 altered significantly. However, a significantly elevated expression was detected for CDC42, CST20, CEK1, and CPH1 in both hyphal forms (Figure 3), while HST7 expression increased only in model hyphae. The adenylyl cyclase (CYR1) pathway in *C. albicans* also functions as a signal integrator for different environmental conditions and is regulated directly by farnesol, CO<sub>2</sub>, glucose and methionine concentration, RAS1, and serum [11] (Figure 3). Expression of almost all components in the CYR1 pathway, such as GPA2, PDE2, TPK1, EFG1, and FLO8, was upregulated in both hyphal forms. Of note, we identified significant induction of EFG1 in both hyphae. EFG1 encodes a transcriptional activator and have a major role in the induction of the hypha-specific genes (Figure 3). FLO8 expression was upregulated in both hyphae, but less, than 2-fold in control.

We also monitored the expression of the major repressors of hypha-specific genes. Slight, but significant increases in expression were observed for RBF1, TUP1 only in model hyphae. Interestingly, we found a moderate increase in the expression of RFG1 in control hyphae, but a robust upregulation was found in model hyphae. NRG1 was slightly upregulated in both hyphae. NRG1 and RFG1 are known to repress transcription of hyphae specific genes, along with TUP1 in response to serum and temperature [69]. Our results suggest that the ratio of transcriptional activators and repressors is crucial in the regulation of the hyphae specific genes, as upregulation of both activators and repressors could be seen (Figure 3).

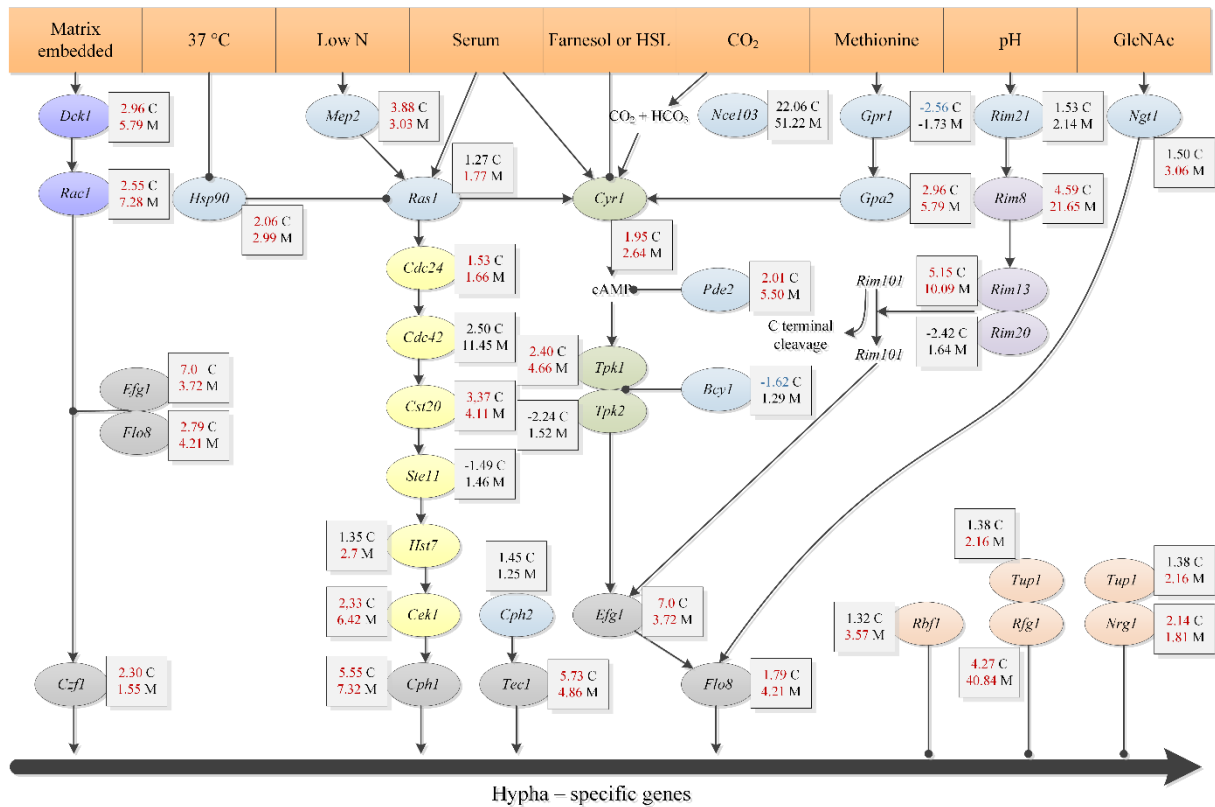


**Figure 3** Comparison of gene expression of signal transduction pathways and their components in vitro. Figure was redrawn from Sudbery [11]; genes are shown with gene names. Numbers show fold change of expression between control hyphae and yeast (C), and model hyphae and yeast (M). Non-significant changes (DEGSeq) in gene expression are marked by black characters; upregulation is marked by red characters and downregulation is marked by blue characters.

N-acetyl-glucosamine (GlcNAc) is known to induce hyphal morphogenesis [70] and white opaque switching [71,72] in *C. albicans*. Interestingly, we found that the NGT1 gene representing the transporter gene in the GlcNAc transporter was solely significantly upregulated in model hyphae, indicating the specificity of this response to epithelial cells (Figure 3).

We have identified a parallel upregulation of several hyphal induction pathways at the level of transcription both in the control hyphae and in hyphae induced by PK E6/E7. Some environmental factors with role in induction, such as glucose concentration and pH, were measured in order to register differentially changing environmental factors in the two hyphae, which could cause bias in the comparison of the two hyphal forms. We found, that pH reduced from 8.0 to  $7.6 \pm 0.04$  in control hyphae and to  $7.6 \pm 0.02$  in model hyphae. Glucose concentration was also reduced from 5.2 mM to 4.58 mM and 4.6 mM in control and model hyphae, respectively. These data show, that both pH and glucose concentration changed in a

similar way and extent in our in vitro system. These values are, however, still in the range, where yeast to hyphae transition of *C. albicans* is strongly induced [73,74].

#### 6.4.2. Expression analysis of genes involved in GlcNAc metabolism

As GlcNAc induces hyphal morphogenesis in *C. albicans* [75], we sought to monitor the expression of GlcNAc catabolic genes in our in vitro model. Since the RNA-Seq experiment did not provide sufficient number of unique reads for statistical analysis of this group (data not shown), the expression of several GlcNAc catabolic genes was tested by QRT-PCR. For this, the following conditions were used: control hyphae, model hyphae, and control hyphae supplemented with 10 mM of GlcNAc. Expressions of GlcNAc deacetylase (DAC1), hexokinase 1 (HXK1) and GlcNAc deaminase (NAG1) were all repressed in control hyphae as compared to the yeast form *C. albicans*; the expression of NGT1 remained unaltered (Figure 4).

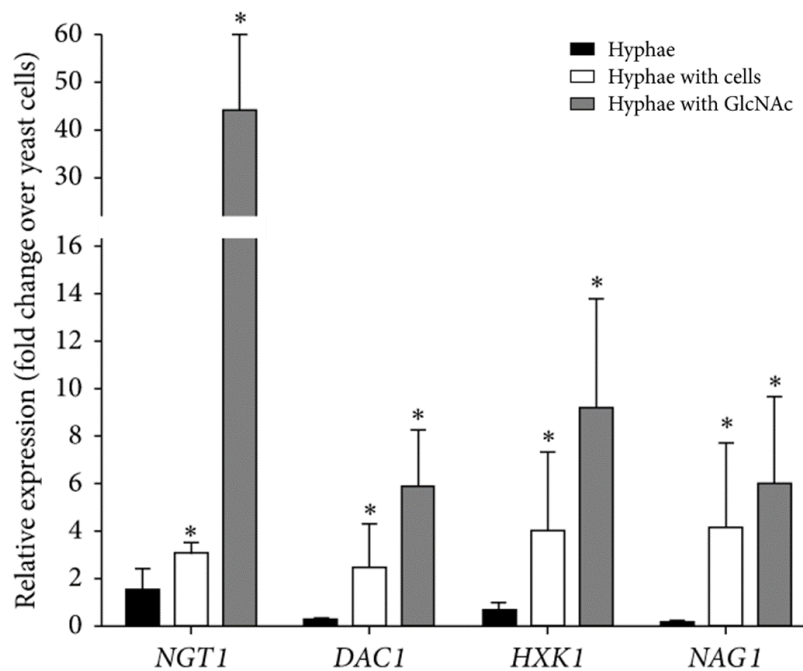


**Figure 4** QRT-PCR analysis of the expression of GlcNAc metabolism genes. The relative gene expression of selected genes shows altered expression upon hyphae development as compared to yeast-like growth. First column (black bars) represents control hyphae; the second (open) and third (gray) columns stand for model hyphae and control hyphae + 10 mM of GlcNAc, respectively. Data are representative of 3 independent experiments and are presented as mean  $\pm$  SD. \*  $p < 0.05$

Lack of induction of these three genes may be due to the fact that these cells were cultured in a mammalian culture medium containing glucose. These results are in agreement

with a previous report, which showed that glucose did not significantly induce the expression of GlcNAc catabolism genes [14]. Furthermore, our results showed that the expression of all four genes (NGT1, DAC1, HXK1, and NAG1) genes involved in GlcNAc catabolism were all significantly upregulated in model hyphae and upon GlcNAc induction (Figure 4). Administration of 10 mM GlcNAc caused definite expression of the GlcNAc catabolic genes that is probably due to the high concentration of the substrate for catabolism (Figure 4).

#### 6.4.3. Virulence of *HXK1* mutant *Candida albicans* is decreased

We next sought to determine the importance of the GlcNAc metabolic pathway in the virulence of the fungus. Taking into account the genes involved in the GlcNAc catabolic pathway, many deletion mutants, such as *ngt1* $\Delta$ , *hvk1* $\Delta$ , *nag1* $\Delta$ , and *dac1* $\Delta$ , have a similar phenotype [49]; However *nag1* $\Delta$  and *dac1* $\Delta$  mutants could not grow on glucose if the medium contained GlcNAc [49]; hence we have chosen to use a *hvk1* $\Delta$  mutant strain in our subsequent experiments. We used an RTCA assay, which provides real-time, quantitative information about the number of the living, attached cells by measuring electrode impedance. Vaginal epithelial cells were treated with different numbers of yeast form *C. albicans* parental (DIC185) or mutant (*hvk1* $\Delta$ ) strains, the impedance was measured for 24 hours and the data was converted to cell index (CI). Microscopic examination showed that both *hvk1* $\Delta$  and DIC185 strains behaved similarly in terms of germ tube formation and germ tube length in all inoculum concentrations during the experiment (data not shown). Our results showed, that the CI of non-treated cells slightly increased, while cells treated with Triton X-100 rapidly detached from the plate surface because of massive cell lysis (Figure 5). When PK E6/E7 VECL cells were infected with low numbers (2000 and 5000) of *C. albicans*, the *hvk1* $\Delta$  mutant exhibited lower cytotoxicity as compared wild type (Figures 5a and 5b). When the number of infecting *C. albicans* cells was increased (10000 and 20000 cells), the *hvk1* $\Delta$  mutant no longer exhibited a reduced cytotoxic effect (Figures 5c and 5d). We also determined, that the cytotoxic effect exhibited by wild type *C. albicans* increased with the cell number used for infection (Figures 5 and 6). Finally, when 2000 yeast cells were used for infection, the CI of vaginal epithelial cells infected with the *hvk1* $\Delta$  mutant was significantly higher at 16, 20, and 24 hours post infection as compared to the control DIC185 strain (Figures 6b, 6c, and 6d, resp.). At increasing *C. albicans* cell numbers used for infection, we only measured a significantly higher cell index of the *hvk1* $\Delta$  mutant at 16 hours post infection (5000 cells; Figure 6b).

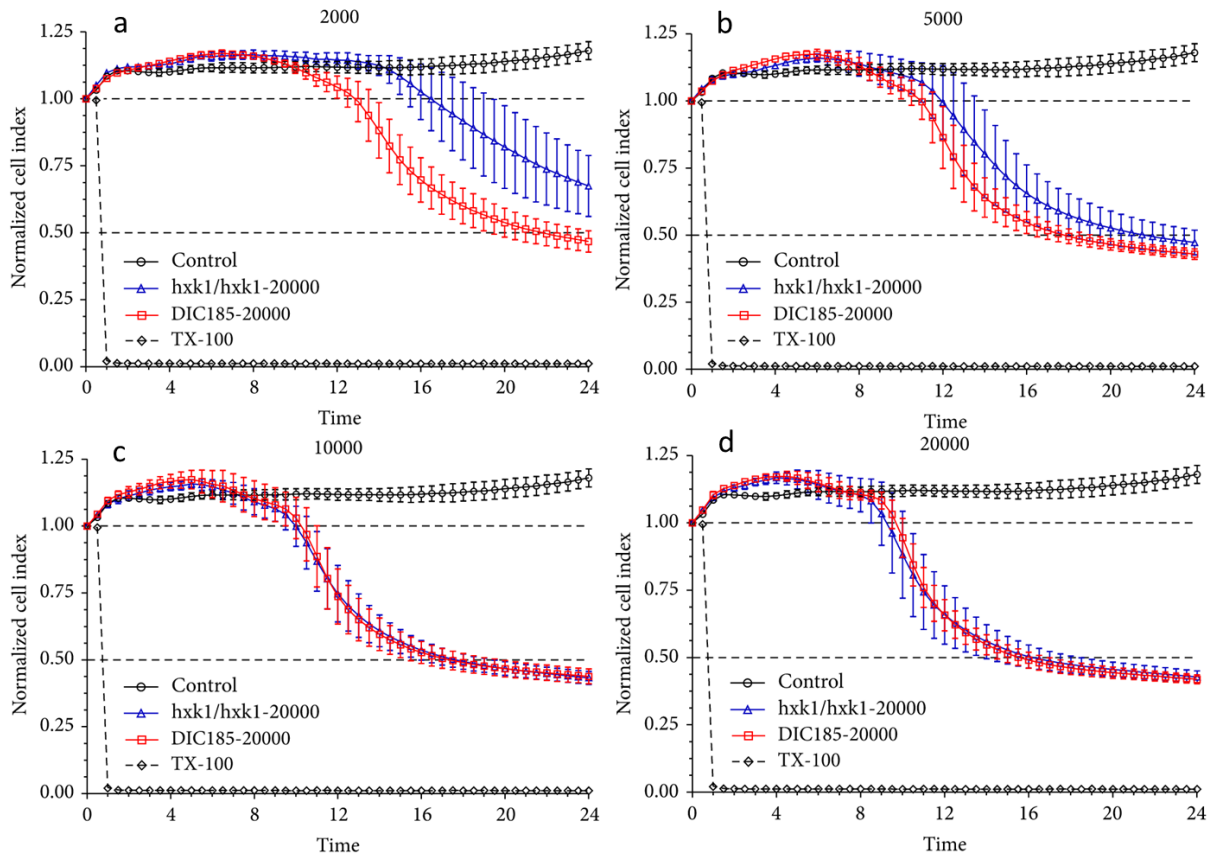


**Figure 5** Effect of *C. albicans* parental (DIC185) and *hxx1* $\Delta$  mutant (*hxx1/hxx1*) strains on the viability of PK E6/E7 vaginal epithelial cells. Cell index (CI) was measured using the RTCA method by xCELLigence System. CI was plotted as a function of time post infection. Different numbers of yeast form *C. albicans* were used as inoculum: (a) 2000 cells/well, (b) 5000 cells/well, (c) 10000 cells/well, and (d) 20000 cells/well.

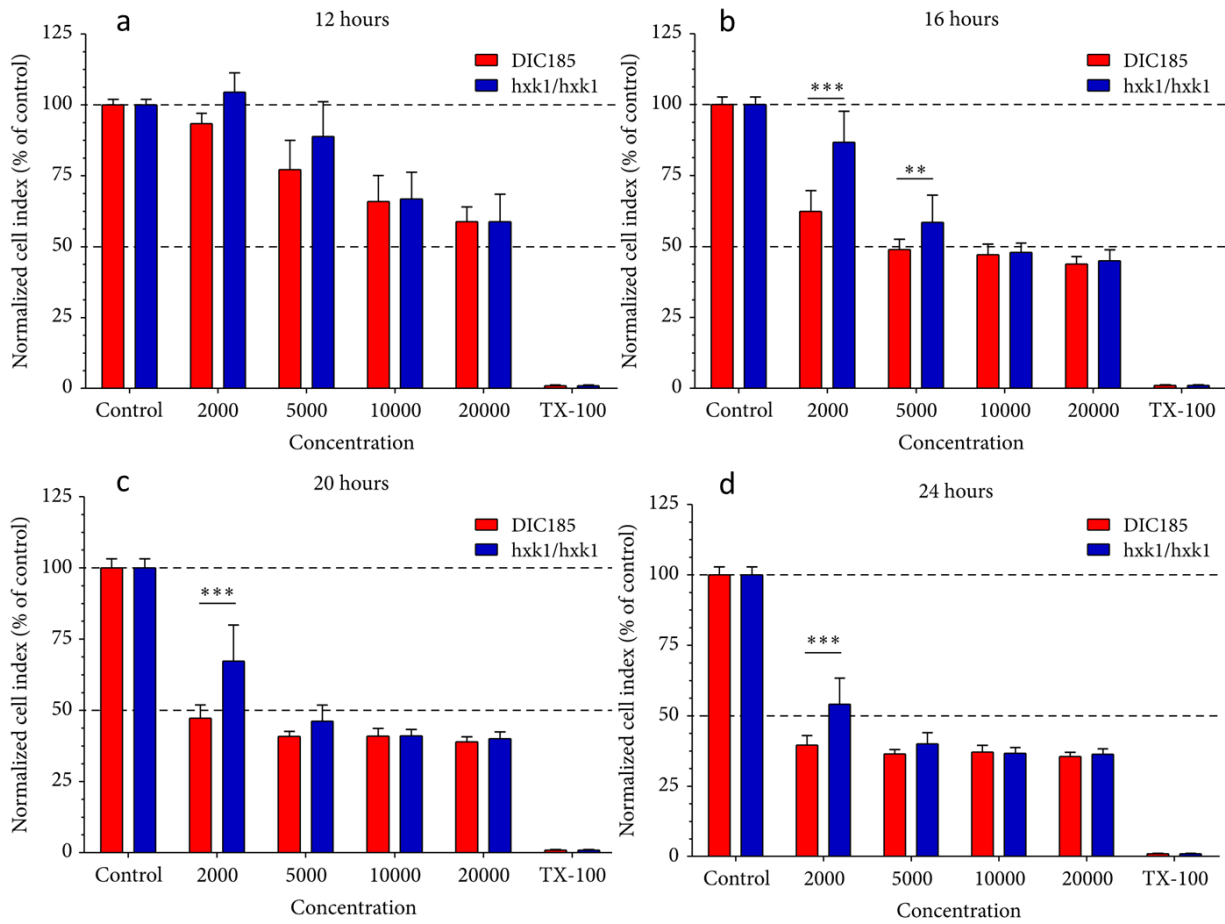


**Figure 6:** Statistical analysis of the RTCA viability test. Cell indexes reflecting viability of PK E6/E7 vaginal epithelial cells infected with the same number of *C. albicans* parental (DIC185) and *hck1* $\Delta$  mutant (*hck1/hck1*) strains were compared. Cell indexes were plotted as a function of inoculum size. Changes were considered statistically significant at  $p < 0.05$  (\*);  $p < 0.01$  (\*\*); and  $p < 0.001$  (\*\*\*)

#### 6.4.4. *GlcNAc* is involved in the adherence of *C. albicans* to vaginal epithelial cells

Numerous published data prove, that *GlcNAc* has a significant role in cell wall construction [76]. We hypothesized, that cell wall, and glycosylated cell wall proteins may have a key role in the adhesion to host cells and this could be an important factor in the decreased virulence of *hck1* $\Delta$  strain. To determine if the *GlcNAc* pathway is involved in the attachment of *C. albicans* to the surface of vaginal epithelial cells, we carried out an adherence assay. Monolayers of PK E6/E7 vaginal epithelial cells were treated with  $3 \times 10^5$  yeast form *C. albicans* parental (DIC185) and mutant (*hck1* $\Delta$ ) strains. After 90 min of contact, which is enough for *C. albicans* cells to form hyphae, non-adhered cells were washed away and the numbers of adherent *C. albicans* cells were counted. Our results showed, that significantly less

hvk1 $\Delta$  mutant remained attached to the surface of the PK E6/E7 cells compared to the DIC185 parental strain (Figure 7). This data indicates the importance of HXK1 gene and therefore the GlcNAc pathway in the adherence of *C. albicans* to vaginal epithelial cells. Noteworthy, it was published parallel with us, that GlcNAc could have a role in adhesion in other organisms, such as *Staphylococcus aureus* [77].

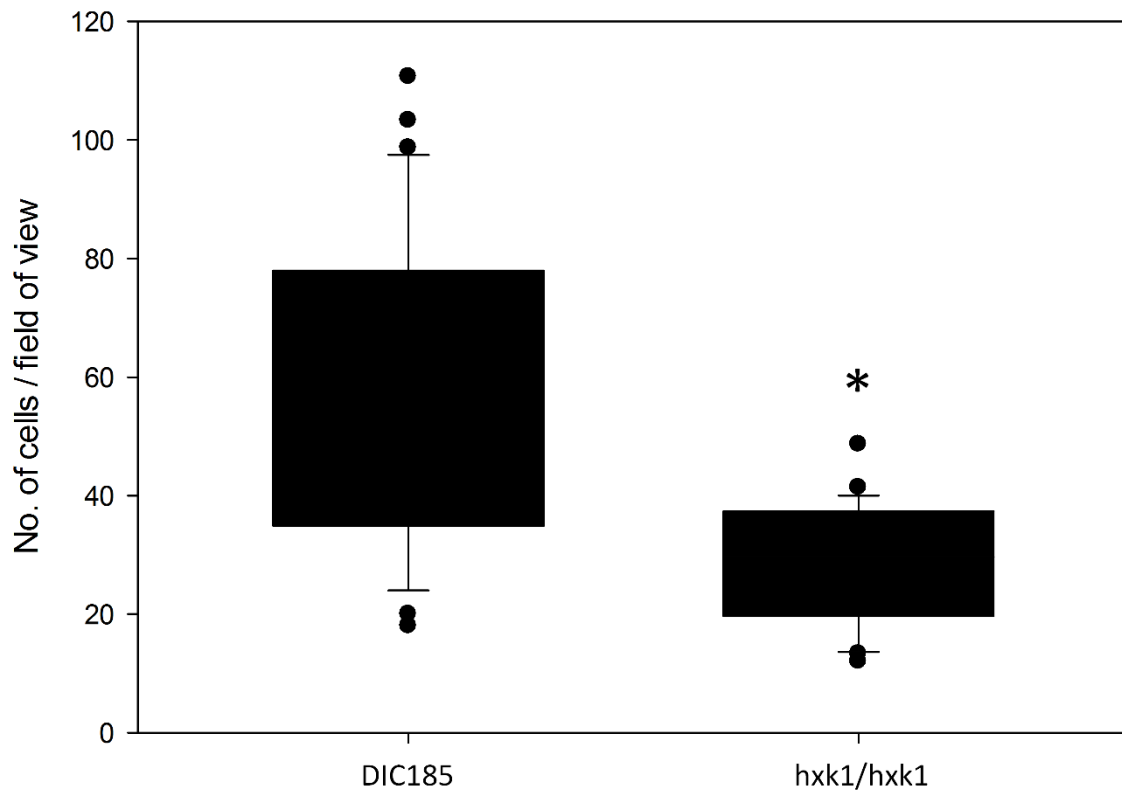


**Figure 7** Adherence of the *C. albicans* parental strain DIC185 and hvk1 $\Delta$  mutant to PK E6/E7 vaginal epithelial cells. The y-axis represents the number of *C. albicans* cells, which remained adhered. The significance of differences between sets of data was determined by two-sample *t*-test; \* $p < 0.05$ .

## 7. Results II

### 7.1. Detection of DEGs with microarray meta-analysis

In order to get reliable data about gene expression in lesional psoriatic skin samples, microarray meta-analysis was carried out. The study by Johnson-Huang et al. was already excluded after sample quality analysis with arrayQualityMetrics package, because at least two samples from one phenotype group are needed for MetaQC analysis and only one non-lesional sample remained after sample filtering. The overall quality of each study was assessed with MetaQC as described before [56]. The software calculated six quality control (QC) measures, then created principal component analysis biplot and standardized mean rank summary score to help in the identification of problematic studies. All five studies were defined as being non-problematic based on quality values (Table 1). DEGs were identified by MetaDE [58]. 2307 upregulated and 3056 downregulated genes were found in lesional skin samples compared to non-lesional ones. DEGs were used for network construction. The high number of DEGs (5363) in our study may be surprising, but it can be caused by the lower gene expression fold change cutoff (1.5 and -1.5 instead of 2 and -2) and by pre - filtering of samples, which can decrease variance and, thus, can increase the number of DEGs.

Study	GEO ID	Platform/Chip	NL	L	IQC	EQC	CQCg	CQCp	AQCg	AQCp	Rank
Gudjonsson et al.[78]	GSE13355	GPL570/Affymetrix HU133 Plus 2.0	54	53	4.18	4	307.65	307.65	95.2	292.19	2.17
Yao et al.[79]	GSE14905	GPL570/Affymetrix HU133 Plus 2.0	27	32	5.58	4	307.65	307.65	81.32	185.34	2.67
Zaba et al.[80]	GSE11903	GPL571/Affymetrix HU133A 2.0	15	12	7.34	3	307.65	307.65	79.24	260.95	2.75
Suarez-Farinas et al.[81]	GSE30999	GPL570/Affymetrix HU133 Plus 2.0	79	80	0.86*	4	307.65	307.65	33	193.93	3.67
Reischl et al.[82]	GSE6710	GPL96/Affymetrix HU133A	12	12	2.7	4	307.65	271.23	40.3	118.68	3.92
Johnson-Huang et al.[83]	GSE30768	GPL571/Affymetrix HU133A 2.0	1	4	Excluded by Array Quality Metrics package						

**Table 1.** Study information and QC measure summary. All studies were carried out on Affymetrix platforms. Asterisks indicate non-statistical significance of QC measures. More non-significant QC measures suggests potentially problematic studies. Study no 6 was already excluded by sample filtering with arrayQualityMetrics. Other studies had high quality and no outlier study was present. IQC: Internal Quality index, EQC: External Quality index, CQCg and CQCp: Consistency Quality Control indexes, AQCg and AQCp: Accuracy Quality Control indexes, NL: non-lesional sample count, L: lesional sample count



## 7.2. General Network analysis

Undirected and directed PPI networks with DEG – coded proteins, directed PDI networks with DEG – coded TFs and regulated DEGs and merged directed networks containing both PPIs and PDIs were created. A TF-TF network consisting of DEG-coded TFs was also generated. The Cytoscape plugin NetworkAnalyzer calculated main network properties for both DEG-derived and control complete networks (Table 2).

Network	Nodes	Edges	Diameter	Average shortest path
<b>PPI Undirected</b>	1614 (9412)	5156 (55039)	14 (12)	4.79 (4.45)
<b>PPI Directed</b>	464 (4040)	815 (13377)	14 (12)	5.26 (4.35)
<b>PDI</b>	2840 (15839)	6398 (123210)	10 (7)	3.69 (3.029)

**Table 2** Results of general network analysis. DEG derived and control networks has similar attributes, but average shortest path length and network diameter is higher in DEG derived networks, which can be explained by lower connectivity (Figure 8). Values for control networks are in brackets.

DEG – derived networks had higher diameter (i. e. the length of the longest shortest path in the network) and average shortest path length, than control full networks. This may be caused by the inverse correlation of node degree and fold change [84]. Nodes with lower fold change has higher degree. As genes with a fold change under cutoff are filtered out from DEG derived networks (between red lines on Figure 8), remaining nodes has smaller average degree, therefore connectivity of the network is lower resulting in higher diameter and average shortest path length value.

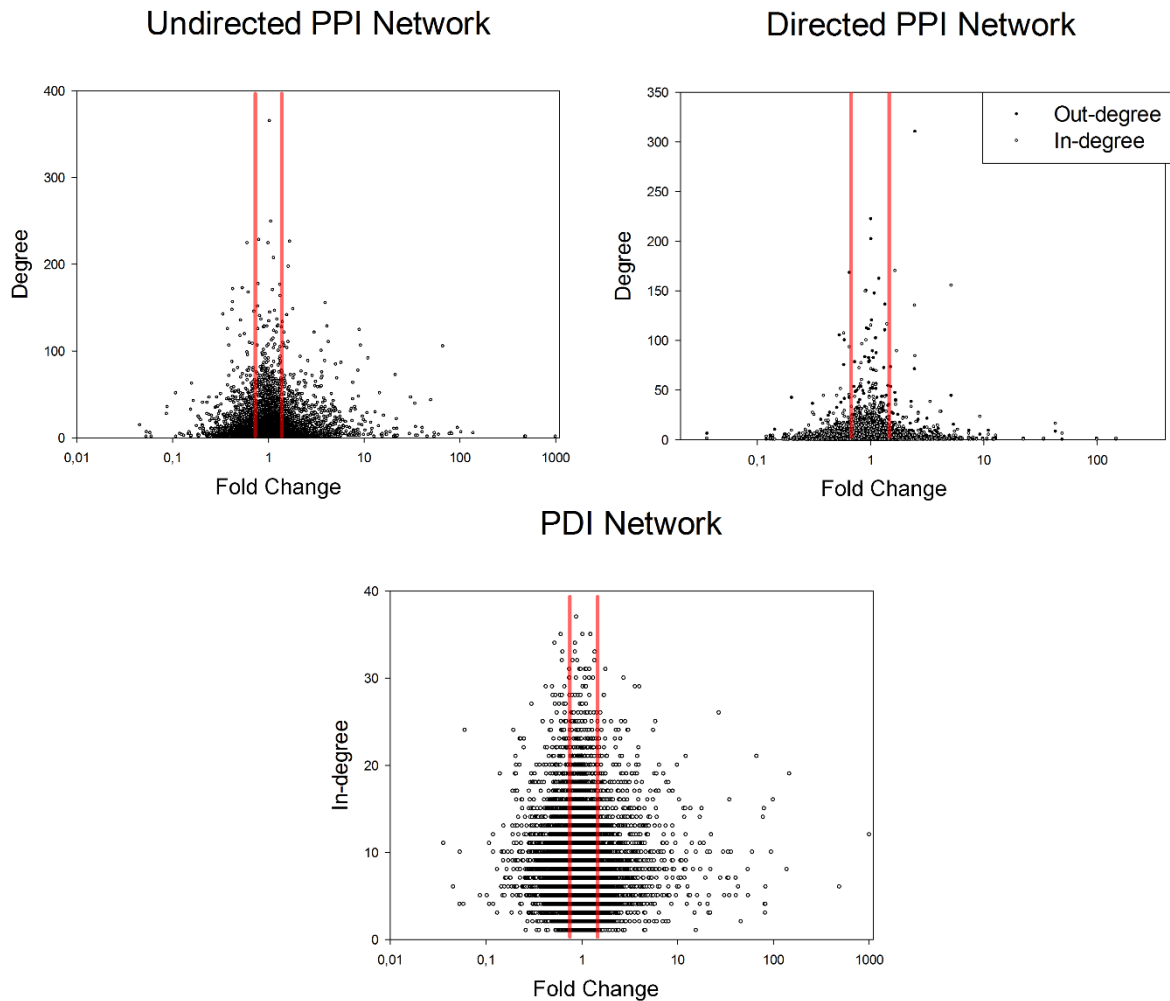


**Figure 8** Degree-Fold Change relationship. Nodes with higher degree has lower fold change of gene expression in all network types. Genes between red lines have higher average degree and are filtered out from network analysis. Remaining nodes in DEG-derived networks have lower average degree and connectivity.

### 7.3. Determination of hubs in DEG-derived networks

Most important nodes of DEG-derived networks were determined using degree and/or stress centralities. Numerous psoriasis-associated protein-coding genes, which are already published, were found (Table 3). CCNA2, FYN and PIK3R1 proteins are yet unpublished in association with the disease and can be found in top rated hubs in undirected PPI network. PDI network contained DEG-coded TFs and regulated DEGs as nodes and directed edges pointing from the TFs to the regulated genes. TFs were ranked using the out-degree centrality. Androgen receptor (AR), TFDP1, MECOM and MEF2A were TFs above centrality cutoff, which are yet not associated with psoriasis.

PPI Undirected		PPI Directed		PDI	
Name	Fold change	Name	Fold change	Name	Fold change
IL8	67.31	IL8	67.31	<b>TFDP1</b>	4.61
CCNB1	11.13	BIRC5	9.3	<b>MECOM</b>	1.7
BIRC5	9.3	MMP1	7.45	<b>AR</b>	-1.65
STAT1	9.04	SOD2	7.2	NF1	-1.71
<b>CCNA2</b>	8.74	IL1B	4.29	<b>MEF2A</b>	-1.74
CXCR4	5.11	STAT3	3.97		
IL1B	4.29	MMP9	3.66		
MAPK14	4.15	SOCS3	3.32		
STAT3	3.97	HMOX1	3.21		
MMP9	3.66	CCL2	2.9		
LCK	3.61	BAX	1.9		
AURKB	2.49	ICAM1	1.72		
MAPK1	1.82	CD69	1.72		
MYC	1.69	MYC	1.69		
NFKB1	1.64	CD86	1.68		
PCNA	1.62	CD28	1.64		
CDKN1A	1.58	NFKB1	1.64		
HDAC1	1.58	EGFR	-1.61		
CYP1A1	-1.6	CTNNB1	-1.65		
EGFR	-1.61	FN1	-1.75		
CREBBP	-1.63	EDN1	-1.84		
CTNNB1	-1.65	SP1	-1.92		
FN1	-1.75	<b>CTGF</b>	-2.04		
<b>FYN</b>	-1.85	NFATC1	-2.19		
SP1	-1.92	IRS1	-2.28		
SMAD4	-1.95	INS-IGF2	-2.33		
INS-IGF2	-2.33	CCND1	-2.34		
CCND1	-2.34	FOS	-2.36		
FOS	-2.36	PPARG	-2.56		
PPARG	-2.56	BCL2	-2.63		
BCL2	-2.63	<b>F3</b>	-3.83		
<b>PIK3R1</b>	-2.96	LEP	-6.27		

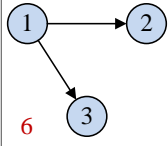
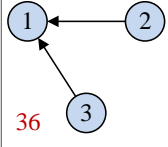
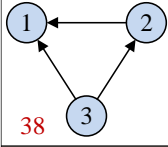
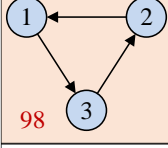
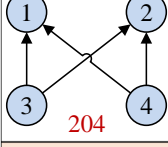
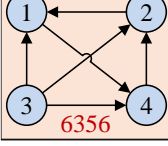
**Table 3** Top rated nodes in DEG-derived networks. Central proteins with centrality value(s) above cutoff are listed. Fold change values between gene expression in lesional and non-lesional samples are also shown. Proteins with bold characters are yet non-published in terms of psoriasis.

#### 7.4. Motif analysis in DEG-derived networks

Motifs consisting of 3 or 4 nodes were analyzed in directed DEG-derived and control networks as well (Table 4). Analysis found motifs, which were enriched in directed DEG-derived but were absent from control networks or vice versa. Some were already generally described in biological systems like convergent (no. 36), divergent (no. 6) and bifan (no. 204) motifs.

An interesting result of motif analysis is the enrichment of feedback loops (no. 98) in merged networks (PDI + PPI), but not in simple ones and the enrichment of motif no. 6356 in

DEG-derived merged network compared to control. Motif no. 6356 consist of a feedback loop and all nodes of the loop are controlled by another separated node.

	PPI directed		PDI		PDI +PPI	
	Psoriasis	Full	Psoriasis	Full	Psoriasis	Full
	0.705	<b>0.031</b>	0.168	0.974	0.908	0.952
	0.997	0.972	0.826	<b>0.023</b>	0.083	<b>0.045</b>
	<b>0</b>	<b>0</b>	0.073	0.978	0.941	0.998
	0.329	0.242	0.518	0.233	0.064	<b>0.046</b>
	0.255	<b>0</b>	0.483	0.082	0.872	<b>0.041</b>
	<b>0.025</b>	<b>0.02</b>	N/A	0.916	<b>0.001</b>	0.512

**Table 4** Summary of network motif analysis Numbers are p values of motif enrichment compared to 1000 random networks. Values with bold red characters are below 0.05 and thus significant.

### 7.5. Controller sub-network construction

Both lesional and non-lesional skin areas can be found on patients at the same time. We wanted to highlight nodes which may be important in the “all or none” switch in lesional skin areas and sustain this phenotype for a long time. To do this, we considered the following: It is reported, that positive feedback loops have fundamental role in maintaining autoimmune and autoinflammatory disease states [85]. It has also been argued that hubs can be found in much more positive feedback loops than negative ones [86]. This is published that in biological

systems, interlinked slow and fast positive feedback loops allow systems to convert graded inputs (like several environmental and genetic factors in a psoriatic individual) into decisive all or none outputs (like lesional skin phenotype) [85,87]. Enrichment of feedback loops (no. 98) and motif no. 6356 (consisting of a feedback loop with all nodes controlled by a separated one) also suggests central role of feedback in lesional skin.

In order to find the most important positive feedback loops containing 2, 3 or 4 nodes, a merged PPI and PDI network was constructed from proteins with centralities above cutoff value. All feedback loops were identified with NetMatch. A positive feedback loop was selected if and only if expression of all nodes changed in the direction of sustaining or suppressing the activity of the loop and „activation” or „inhibition” properties of all edges were proven by publications. Expression of all nodes was downregulated in two loops having role in carbohydrate metabolism: the INS-IGF2-EDN1-LEP-INS-IGF2 and the LEP-PPARG-INS-IGF2-LEP loop. The IL1B-NFKB1-CCL2-IL1B loop contained only upregulated nodes and has role in inflammation (Figure 10). The remaining loops contained inflammation and metabolism-related nodes as well. These may be key components in the metabolic-inflammatory interplay in the pathomechanism of psoriasis. All positive feedback loops had common nodes, thus a merged network was generated containing interlinked positive feedback loops (Figure 10). Transcriptional changes of all nodes and influence of all edges supported the sustainment of lesional phenotype in this sub-network, which has been proven by Boolean analysis (Table 5).

	Input state	Relation	Future state(*)
<b><i>NFATC* = FOS</i></b>	0	0	0
<b><i>FOS* = EDN1</i></b>	0	0	0
<b><i>EDN1* = NFATC1 and INS-IGF2 and LEP</i></b>	0	0 and 0 and 0	0
<b><i>INS-IGF2* = PPARG and LEP</i></b>	0	0 and 0	0
<b><i>LEP* = EDN1 and INS-IGF2</i></b>	0	0 and 0	0
<b><i>PPARG* = INS-IGF2 and LEP and AR</i></b>	0	0 and 0 and 0	0
<b><i>AR* = not (IL8 and NFKB1)</i></b>	0	not (1 and 1)	0
<b><i>STAT3* = not AR</i></b>	1	not 0	1
<b><i>IRF1* = STAT3</i></b>	1	1	1
<b><i>IL8* = not PPARG; STAT3 and IRF1 and NFKB1</i></b>	1	not 0; 1 and 1 and 1	1
<b><i>IL1B* = CCL2</i></b>	1	1	1
<b><i>NFKB1* = not AR; IL1B</i></b>	1	not 0; 1	1
<b><i>CCL2* = NFKB1 and IL1B</i></b>	1	1 and 1	1

**Table 5. Boolean analysis of controller network** Logical relations can be seen in the first and third column. Input and future state of network is stationary

Nodes with downregulated expression got value of 0 and nodes with upregulated expression got value of 1. Future state of nodes was set based on interactions (Table 5). The output Boolean values were the same as the input state suggesting constant future state of the system and, thus, the sustainment of lesional phenotype.

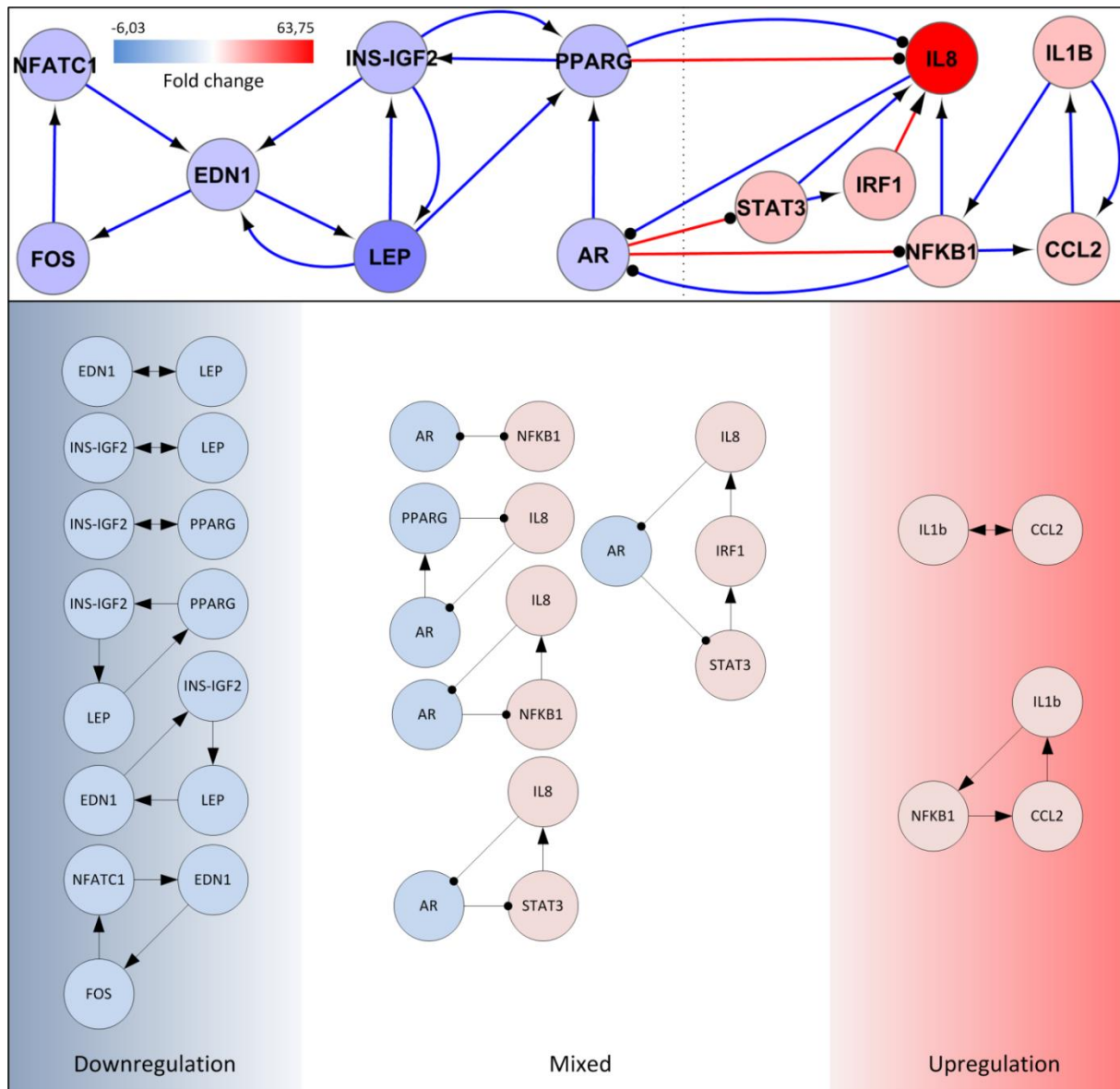


**Figure 10** Positive feedback loops and the merged controller sub-network in lesional psoriatic skin. Individual positive feedback loops with 2, 3 or 4 nodes are shown. Node color is blue if the gene expression is decreased and red if increased is lesional skin samples. Merged controller sub-network is shown on the top. Node color is proportional with fold change values. red line: gene regulatory interaction; blue line: protein-protein interaction; arrow-headed line: activation; bar-headed line: inhibition

## ***7.6. Analysis of chemical-protein interaction networks***

Undirected and directed chemical-protein interaction networks were constructed using STITCH database, which contained interactions between proteins and chemical compounds (internal non-protein substances, drugs and environmental substances) [61]. Drugs or potential drugs were filtered out from chemicals and ranked by degree and stress centrality in case of undirected and out degree centrality in case of directed networks. Top ranked drugs were grouped into Anatomical Therapeutic Chemical (ATC) classes (Table 6) [88]. KEGG DRUG was used for classification [89]. Results showed a big overlap between undirected and directed network analysis. Best rated drugs were retinoic acid, cholecalciferol, corticosteroids, methotrexate, sirolimus and tacrolimus, which can be already found in psoriasis guidelines and large clinical trials have proved their effectiveness [90].

Psoriasis studies are available for numerous potential drugs with high centralities. “Blood glucose lowering drugs” are promising drug candidates. The biguanide metformin in this group is associated with reduced psoriasis risk in a population based case control study [91]. Many studies are available about “Thiazolidinedione” antidiabetic drugs. A recent meta-analysis showed significant decrease in Psoriasis Area and Severity Index (PASI) scores compared to placebo in case of pioglitazone and non-significant improvement in PASI 50/70 in case of rosiglitazone [92]. Troglitazone normalized histological features of psoriasis models and the lesional phenotype in a small clinical trial [93]. The “HMG CoA reductase inhibitor” drug simvastatin was effective in a pilot study, although atorvastatin in the same class showed only a non-significant improvement in a different study [94,95]. Salicylic acid has antifungal effects and it’s used as an adjuvant because of its keratolytic effect in the treatment of psoriasis [96]. The “Antineoplastic agent” methotrexate is a well-known medication for psoriasis. Several additional drugs in the same class were found in our analysis: studies are available for 5-fluorouracil in the treatment of dystrophic psoriatic fingernails, but it showed only non-significant improvement [97]; micellar paclitaxel significantly improved psoriasis in a prospective phase II study [98]. A study reported significant effectiveness of topical caffeine [99]. The “Calcium channel blocker” nifedipine is found to be an inductor of the disease in a case control study [100]. A study in 2005 reported significant PASI score reduction of 49.9% by topical theophylline ointment [101]. Mahonia aquafolium extract - containing berberine among others - is not classified into ATC classes, but three clinical trials already indicated improvement of psoriasis with the use of this substance [102]. Multiple studies prove efficacy of the terpenoid triptolide in the treatment of psoriasis [103]. A recent study investigated the

effect of rifampicin on psoriasis and reported a 50.03% mean PASI reduction [104]. A study about the treatment of psoriasis with curcumin was carried out, but reported only low response rate [105].

The efficacy of several drugs in results are supposed by in vitro experiments. The “Lipid modifying agent” clofibrate, but not bezafibrate reversed UVB-light-mediated expression of psoriasis – related inflammatory cytokines (IL6, IL8) [106]. Fluvastatin and pravastatin have the potential to inhibit Th17 cell chemotaxis, thus lowering immune cell infiltration of psoriatic skin [107]. Anti-proliferative effect of novel COX2 inhibitors on HaCaT keratinocytes was proven in an in vitro experiment and possible therapeutic use in psoriasis was supposed [108]. However, no such experiment was carried out with celecoxib which was the only COX2 inhibitor in our results. N-acetyl-cysteine attenuated TNF alpha – induced cytokine production in primary human keratinocytes, which suggests its anti-psoriatic potential [109]. The “Thiazolidinedione” ciglitazone was never used as a drug, but inhibited keratinocyte proliferation in a dose dependent fashion [93]. Histone – deacetylase inhibitor trichostatin A blocked the conversion of regulatory T cells to IL17-expressing T cells suggesting its beneficial role in treating psoriasis [110]. Tse et al. supposed, that antiproliferative effect of arsenic compounds could have positive effects on psoriatic skin [111]. The phosphodiesterase inhibitor rolipram has the ability to block enterotoxin B-mediated induction of skin homing receptor on T lymphocytes and may have the potential to inhibit lymphocytic infiltration of lesional skin [112]. The natural polyphenolic compound rottlerin is a potent inhibitor of NFκB and may have disease modulating effects [113].

Case reports are available about psoriasis induction by clonidine, two “agents acting on the renin-angiotensin system” like captopril or losartan; the “protein kinase inhibitor” and “antineoplastic agent” imatinib; diclofenac, olanzapine, fluoxetine and chloroquine. Also case reports are available about the beneficial effects of ritonavir; “antineoplastic agents” like cytarabine, doxorubicin, and cisplatin; gefitinib, colchicine, lidocaine and nicotine [114-128].

In summary, studies are available for 34 drugs, experimental evidence is available for 24 drugs, case reports suggest beneficial or disease-inductor effect of 21 drugs and we also found 98 unpublished drug candidates for the treatment of psoriasis (Table 6-7).



<b>ATC Class</b>	<b>Drugs</b>
<b>STUDIES AVAILABLE</b>	
<b>Retinoids for topical use in acne</b>	retinoic acid
<b>Corticosteroids</b>	dexamethasone, hydrocortisone, corticosterone, prednisolone
<b>H2 receptor antagonists</b>	cimetidine
<b>Immunosuppressants</b>	sirolimus, tacrolimus
<b>Antiinflammatory and antirheumatic drugs</b>	indomethacin
<b>Blood glucose lowering drugs excl. insulines</b>	metformin, troglitazone, rosiglitazone, pioglitazone
<b>Intestinal anti-inflammatory agents</b>	sulfasalazine
<b>Vitamins</b>	cholecalciferol, folic acid
<b>Antimycobacterials</b>	rifampicin
<b>Mineral supplements</b>	selenium
<b>Antifungals for topical use</b>	salicylic acid
<b>Antineoplastic agents</b>	5-fluorouracil, methotrexate, paclitaxel, cycloheximide
<b>Cardiac stimulants excl. cardiac glycosides</b>	epinephrine-bitartrate, norepinephrine
<b>Lipid-modifying agents, plain</b>	simvastatin, atorvastatin-calcium
<b>Calcium channel blockers</b>	nifedipine
<b>Psychoanaleptics</b>	caffeine
<b>Thyroid therapy</b>	Liothyronine
<b>Drugs for obstructive airway diseases</b>	theophylline
<b>N/A</b>	berberine, curcumin, triptolide
<b>EXPERIMENTAL EVIDENCE</b>	
<b>Topical products for joint and muscular pain</b>	capsaicin
<b>Respiratory system</b>	N-acetyl-L-cysteine
<b>Antineoplastic agents</b>	Velcade, celecoxib
<b>Hormone antagonists and related agents</b>	tamoxifen
<b>Cardiac stimulants excl. cardiac glycosides</b>	isoproterenol
<b>Liver therapy</b>	glycyrrhizinic acid
<b>Antiinfectives and antiseptics, excl. combinations with corticosteroids</b>	arsenic
<b>Beta blocking agents</b>	propranolol
<b>Lipid-modifying agents, plain</b>	clofibrate, bezafibrate, fluvastatin, pravastatin
<b>Blood glucose lowering drugs excl. insulines</b>	ciglitazone
<b>N/A</b>	N-ethylmaleimide, baicalein, apigenin, SB 202190, monensin, rolipram, eflornithine, calphostin C, trichostatin A, rottlerin
<b>CASE REPORTS</b>	
<b>Antivirals for systemic use</b>	ritonavir
<b>Antiinflammatory and antirheumatic drugs</b>	diclofenac, ibuprofen, aspirin
<b>Antigout preparations</b>	colchicine
<b>Antiprotozoals</b>	chloroquine
<b>Ophthalmologicals</b>	atropine
<b>Antineoplastic agents</b>	cytarabine-hydrochloride, doxorubicin, cisplatin, imatinib, docetaxel, gefitinib
<b>Cardiac stimulants excl. cardiac glycosides</b>	phenylephrine
<b>Antiadrenergic agents, centrally acting</b>	clonidine
<b>Agents acting on the renin-angiotensin system</b>	captopril, losartan
<b>Anaesthetics</b>	lidocaine
<b>Psycholeptics</b>	olanzapine
<b>Psychoanaleptics</b>	fluoxetine
<b>Other nervous system drugs</b>	nicotine

Table 6. Published Drugs

<b>ATC Class</b>	<b>Drug</b>
<b>Retinoids for topical use in acne</b>	retinol
<b>Blood glucose lowering drugs excl. insulines</b>	glyburide
<b>Vitamin K and other hemostatics</b>	menadione
<b>Antineoplastic agents</b>	aldophosphamide, MLS003389283, etoposide, dasatinib, decitabine
<b>Sex hormones and modulators of the genital system</b>	(4-14c)pregn-4-ene-3,20-dione, mifepristone, testosterone-propionate, androstanolone, diethylstilbestrol, raloxifene
<b>Hormone antagonists and related agents</b>	flutamide, fulvestrant
<b>Cardiac stimulants excl. cardiac glycosides</b>	bucladesine
<b>Cardiac glycosides</b>	G-Strophanthin
<b>Drugs for obstructive airway diseases</b>	salbutamol
<b>Antiadrenergic agents, centrally acting</b>	reserpine
<b>Antiadrenergic agents, peripherally acting</b>	prazosin
<b>Lipid modifying agents, plain</b>	lovastatin, pitavastatin, fenofibrate
<b>Calcium channel blockers</b>	verapamil
<b>Diuretics</b>	furosemide, spironolactone
<b>Liver therapy</b>	silibinin
<b>Platelet aggregation inhibitors excl. heparin</b>	dipyridamole, cilostazol, amiloride-hydrochloride
<b>Agents acting on the renin-angiotensin system</b>	telmisartan, valsartan
<b>Anaesthetics</b>	ketamine, propofol, cocaine, isoflurane
<b>Analgesics</b>	morphine
<b>Psycholeptics</b>	haloperidol, clozapine, diazepam
<b>Psychoanaleptics</b>	desipramine, amitriptyline, metamphetamine
<b>Antiepileptics</b>	phenobarbital, valproic acid
<b>Antidotes</b>	naloxone
<b>Other nervous system drugs</b>	carbacholin
<b>N/A</b>	cytochalasin D, aminoguanidine, Neurogard, paraquat, Y27632, oxidopamine, nitroarginine, AC1LA4H9, SL327, emodin, 2,3,7,8-tetrachlorodibenzo-dioxin, 3-(2-aminoethyl)-5-[(4-ethoxyphenyl)methylidene]-1,3-thiazolidine-2,4-dione, ChEMBL248238, geldanamycin, anisomycin, 8-bromocyclic GMP, tempol, MK-801, 1-(5-isoquinolinesulfonyl)-2-methylpiperazine, ionomycin, herbimycin, pyrrolidine dithiocarbamate, nordihydroguaiaretic acid, gamma-imino-ATP, forskolin, GMP-Pnp, roscovitine, flavopiridol, N-formyl-Met-Leu-Phe, ns-398, sodium butyrate, AC1L118V, tyrphostin B42, kainic acid, pirinixic acid, IBMX, bisindolmaleimide I, proline-dithiocarbamate, KBio2_002303, Zillal, thapsigargin, calcimycin, clenbuterol, indole-3-carbinol, 1,9-pyrazoloanthrone, herbimycin, kaempferol, daidzein, lithium-chloride, naringenin

**Table 7.** Drug candidates unassociated with psoriasis

### 7.7. Effective drugs predominantly act on proteins of the controller sub-network

The 32 effective drugs in the “Studies available” group were selected from STITCH data and target proteins were analyzed. All target proteins got an in-degree value reflecting the number of effective drugs acting on it. The group of proteins forming the controller sub-network was compared with the group of other targets. The controller sub-network protein group got significantly higher median value than the other one (10 vs. 1) with Mann-Whitney Rank Sum Test, which prove the importance of the controller sub-network in psoriatic lesions. (Figure 11) Noteworthy, that in-degree has power law distribution, thus T-test could not be used.

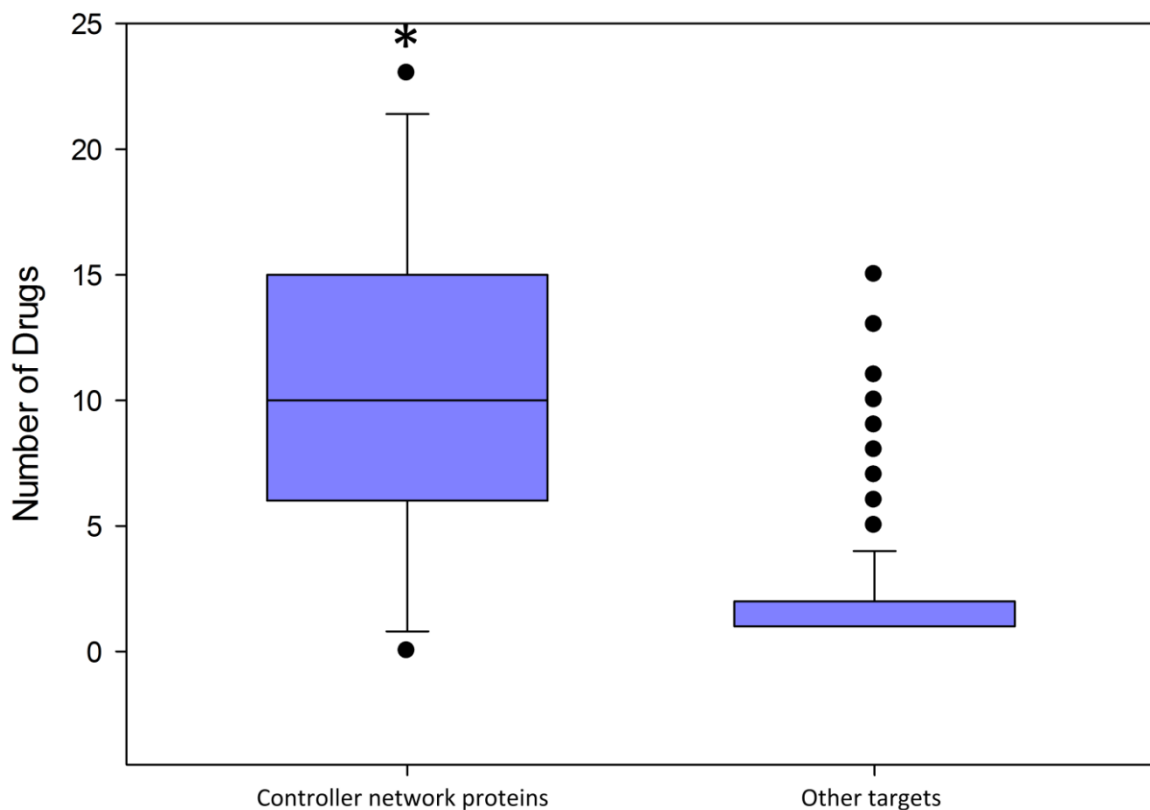


**Figure 11. Effect of anti-psoriatic drugs on controller network.** A larger number of effective anti-psoriatic drugs act on controller nodes than on other proteins. Totally, the targets of 32 effective anti-psoriatic drugs were analyzed (median 10 vs. 1) \* $p < 0.001$

## 8. Discussion

### 8.1. *In vitro* modelling vs. biopsy specimens

#### 8.1.1. Vulvovaginal Candidiasis

We used *in vitro* modelling in our *C. albicans* study. We hypothesized, that although hyphal transition is an obligate step during pathogenesis, many other genes and processes are needed for virulence and, thus, hyphae growing in the presence of human cells may be markedly different from control hyphae, which is triggered only by physical environmental factors. One of the biggest challenge was to model VVC *in vitro* trustworthily.

Secretions of the female genital tract keep the epithelial surface of the vagina moist. The lactic acid concentration of the vaginal fluid creates a pH of approximately 4.5 [129]. However, lactic acid concentration and pH similar to that of the vaginal fluid greatly inhibited cell division and germ tube formation of *C. albicans* in previous reports [130,131]. Thus, in our experimental model, *C. albicans* was cultured in CKM at pH 8.0. Culturing medium contained glucose at 5.6 mM concentration. Glucose concentration of the vaginal fluid contains ~5.2 mM glucose as a final concentration [132]. Our RNA-Seq data showed strong upregulation of the gluconeogenesis, glyoxylate cycle, and fatty acid beta-oxidation pathways in both the control hyphae and hyphae developed in the presence of VECL (data not shown). This is in complete agreement with an earlier report, in which microarray analysis of phagocytosed *C. albicans* cells showed the upregulation of the glucose starvation related metabolic pathways, such as gluconeogenesis, glyoxylate cycle, and fatty acid beta-oxidation [133]. Noteworthy, 0.1% (w/v) glucose (5.6 mM) strongly induced hypha development of *C. albicans* on solid media [74]. Starvation to glucose may be one factor that drives the yeast to hyphae transition of *C. albicans* in our *in vitro* system. Additionally, we used the temperature of the human body (37 C) in our experiments, which also induces filamentation [11].

Although we tried to consider as many factors as possible during *in vitro* modelling, it had some limitations. First, hyphal growth of *C. albicans* is regulated by other microorganisms in the vaginal microbiome with yet unknown mechanisms. Additionally, we do not know the concentration of *C. albicans* cells relative to human cells *in vivo*, thus we used only empirical MOI. We used only one human cell type in our *in vitro* system, although there are numerous cell types *in vivo*. Though these drawbacks mentioned before, with the use of adequate controls (control hyphae and yeast), we were able to find important factors in the fungal-host interaction.

### 8.1.2. Psoriasis

Several microarray studies were available for our *in silico* analysis of psoriasis. All of them assessed gene expression of punch biopsy specimens. Biopsy specimens are suitable for the investigation of complex diseases like psoriasis. Although the phenotype can be analyzed with its own complexity, there are also drawbacks available. First, in case of *in vitro* modelling, standardization is relatively easy, but in case of biopsy specimens it is cumbersome. We can select patients of the same age, gender, disease severity, treatment, but there can be numerous personal variations, which may have significant influence on gene expression. The goal of microarray meta-analysis is to avoid these variations and find uniform expression patterns among studies. Second, cellular-level gene expression analysis is difficult. There are *in silico* methods, which are able to determine cell-specific expression data from high throughput data of tissues, but the resolution of results is low and it is sometimes biased [134]. Single cell RNA sequencing is promising, but the dissection of different cell types from tissue specimens is problematic [135].

## 8.2. Filtering data and identification of important genes

### 8.2.1. Vulvovaginal candidiasis

As it could be seen from our two studies, filtering, normalization and the use of biostatistics is essential in high throughput gene expression studies. Although the price of RNA-seq is getting lower, sometimes it is still too expensive to sequence the whole transcriptome separately of three or more biological replicates. As our goal was to identify proteins or processes consisting of several proteins potentially important for the virulence of *C. albicans*, we carried out RNA-seq for the pooled RNA of three biological replicates. The resultant data was capable for the identification of proteins or processes and the findings could be further explained and validated with other *in vitro* methods. As we had only pooled gene expression data for each experimental scenario, special statistical inference was needed for the detection of differentially expressed genes and most important results had to be validated with quantitative real time PCR using biological replicates. Numerous genes with a known role in pathogenesis have been detected in DEGs, but we focused on GlcNAc metabolism and investigated its potential role in adhesion.

### 8.2.2. Psoriasis

The purpose of a meta-analysis is to create general assumptions without the bias caused by geographical, ethnical, gender, study-design or age-related differences. The analysis process

for all microarray study were standardized and strict requirements were set for all of them. They had to be carried out on the same chip or chip family, and be suited to MIAME. We made the normalization and filtering process with the same methods for all studies. Quality assessment of all individual samples in a microarray study was carried out with ArrayQualityMetrics and all low-quality samples were excluded. Low-quality or outlier studies were further filtered with MetaQC. We wanted to construct whole networks from DEGs and make inference about network dynamics, thus, the selection of fold-change cutoff for DEGs was critical. Fold change cutoff selection is usually an empirical process. The same cutoff is chosen for all genes, although the expression range is affected by their function and network centralities [84]. We used the lower fold change cutoff of 1.5 instead of 2 to avoid the exclusion of potentially important proteins and genes. Noteworthy, lot of hubs in our analysis with highest centralities had lower, than 2 absolute fold change value, which can be caused by the negative correlation between degree and gene expression fold change values (Figure 8) [84]. The ideal method would be the selection of cutoff values for each gene individually considering their range of expression, which is already registered in other studies.

We generated PPI networks based on the largest PPI database (STRING) available, which contains experimentally proven interactions as well as highly reliable ones based on prediction algorithms or data mining. PDI network was also generated using not only literally proven interactions but interactions predicted by high fidelity algorithms. The selection of nodes with highest centralities wasn't straightforward too. Degree and stress node centralities represent power law distribution, thus, special statistical considerations were needed. The use of lower DEG fold-change cutoff and detailed analysis based on node centrality statistics made it possible to identify proteins yet not associated with the disease but may have remarkable role in its pathogenesis.

### **8.3. Putting genes in context**

#### **8.3.1. Vulvovaginal candidiasis**

Changes in the microenvironment massively induced many components of several different signal transduction pathways resulted in the morphological transition of *C. albicans* both in model and control conditions, but the GlcNAc transporter NGT1 was induced significantly exclusively in response to vaginal epithelial cells (Figures 3 and 4). We also found that the *hvk1Δ* mutant exhibits reduced cytotoxicity compared to the wild type strain of *C. albicans*, which may be caused by its decreased adherence to the surface of vaginal epithelial

cells (Figures 5 - 7). The human extracellular matrix contains a significant amount of GlcNAc [75]. In agreement with a recent review [75], GlcNAc released from the extracellular matrix of human cells during membrane remodeling might explain the induction of *C. albicans* GlcNAc catabolic genes, such as, NGT1, HXK1, NAG1, and DAC1 (Figure 4) by vaginal epithelial cells.

Adherence to the surface of epithelial and endothelial cells and penetration of hyphae into these cells are important virulence factors contributing to the pathogenesis of *C. albicans* [19]. The GlcNAc biosynthesis plays a key role in chitin biosynthesis [75]. The inner layer of the cell wall of *C. albicans* consists of chitin (polymers of  $\beta$ -(1,3)-glucan,  $\beta$ -(1,6)-glucan, and GlcNAc). This scaffold binds glycosylphosphatidylinositol- (GPI-) anchor-dependent cell wall proteins, which play an important role in the adherence of *C. albicans* to the epithelial cells [11]. This suggest, that decreased adherence in *hxk1* $\Delta$  could be caused by decreased chitin synthesis. This theory is supported by a study, in which Nikkomycin Z, a chitin biosynthesis inhibitor caused reduced adherence of *C. albicans* to the surface of buccal epithelial cells [136].

### 8.3.2. Psoriasis

Keratinocyte hyperproliferation and inhibition of apoptosis are well-known phenomena in psoriasis. Several proteins have been associated with these mechanisms like BCL2, BAX, NFATC1, PPAR $\delta$ , EGF, mTOR, NF- $\kappa$ B etc.[137-140] Most of them could be found in the group of central proteins detected by DEG-derived network analysis. Unpublished DEG-coded proteins with potential role in hyperproliferation, like CCNA2, TFDP1 and MECOM, were also found (Table 3). CCNA2 encodes Cyclin A2, that controls S phase and G2/M transition. A recent study reported that CCNA2 protein has role in cytoskeletal rearrangements and cell migration as well [141]. Not only cell cycle progression is abnormal in lesional skin, but actin cytoskeleton organization as well [142]. Thus, Cyclin A2 may take part in hyperproliferation and in aberrant actin cytoskeleton organization in psoriatic skin keratinocytes. TFDP1 encodes DP1 protein, which is a dimerization partner of the E2F transcription factor. The E2F/DP1 heterodimers regulate cell cycle via DNA replication control and apoptosis. DP1 has E2F-independent function as well: DP1 can stabilize Wnt-on and Wnt-off states in Wnt/ $\beta$ -catenin signaling and determine differential cell fates [143].

Psoriasis is an immune-mediated disease. Some proteins, which are published as important factors in pathogenesis, were absent from DEGs in our microarray-meta analysis. For example TNF alpha was not identified as a hub, although it is an important target in psoriasis

therapy. This could be explained by the finding that increased TNF alpha in psoriatic plaques are caused mainly by post-transcriptional mechanisms [144]. Many proteins published in association with the immunopathogenesis of psoriasis were highly ranked hubs in PPI networks: IL1, IL8, TGFB1, SP1, STAT1, STAT3, NFKB1, IRF1 etc.[139,145-151] The downregulation of the src kinase FYN seems to be a counteracting compensatory mechanism as this protein is important in IFN gamma action, in TNF alpha induced COX2 expression and in adipose tissue - mediated inflammation leading to insulin resistance. These processes are important in the pathomechanism of psoriasis [152-154]. This data is in agreement with our chemical-protein interaction network analysis, which suggests, that the FYN inhibitor KBio2\_002303 may have beneficial effects in the treatment of psoriasis. An important node in controller sub-network is IL8. Although its role in psoriasis pathogenesis is reported, no trial has been done with IL8 inhibitors [155]. This is true for CCL2 and IRF1 as well. Our study confirms their basic role in the sustainment of lesional phenotype as both can be found in highly ranked hubs. CCL2 is also essential in the controller sub – network by activating two positive feedback loops related to inflammation.

Comorbidity of psoriasis and metabolic syndrome is a well-known phenomenon. There is a complicated interaction between the two diseases mediated by inflammatory cytokines among other factors [156]. Numerous DEG-coded proteins associated with both diseases could be found in central proteins like PPARG, INS-IGF2, LEP etc. (Table 3) [157-159] Others, like PIK3R1, AR and MEF2A may have role in the development of metabolic syndrome in psoriatic patients. PI3KR1 is important in the development of insulin resistance, it propagates inflammatory response in obese mice and may be an important link between the obesity-inflammation interplay in psoriasis [160]. AR has important effect on insulin signaling and thus insulin resistance. It is published that AR knockout mice exhibit insulin resistance [161]. To our knowledge, AR has not yet been associated with psoriasis. However it was found in 1981, that lower serum testosterone level therefore decreased AR activation can be detected in psoriatic patients [162]. AR and PPARG connect inflammation- and metabolism-related hubs in controller network. MEF2A is important for GLUT4 expression on insulin-responsive cells. Expression of MEF2A is downregulated in lesional skin samples which suggests another possible mechanism for insulin resistance in psoriasis.

The real purpose of systems biology is to construct models from high throughput data. High precision data is needed for reliability. We used data of gene expression in our psoriasis study. We didn't measure protein abundance and didn't assess allosteric modulation of proteins



or generation of protein complexes. Additionally we didn't have expression data for different time points. Thus, an accurate model with differential equations could not be constructed. However, we were able to detect a sub-network with the use of network motif analysis, which could potentially induce and maintain the lesional phenotype of the disease.

#### **8.4. Therapeutic aspects**

Chemical – protein interaction networks were created using STITCH database and we managed to predict disease – modifying drugs. Many drugs, which are already widely used in the treatment of psoriasis could be found as highly ranked nodes in chemical-protein interaction networks such as methotrexate, retinoic acid, corticosteroids, sirolimus and tacrolimus (Table 6). According to STITCH data, all of them act on at least one of the hubs in the controller sub-network. Members of highly ranked ATC classes also target proteins in the controller sub-network. Blood glucose-lowering drugs act through PPARG and INS-IGF2 activation and fibrate and HMG-CoA inhibitors may improve psoriasis through the modulation of these proteins as well [92]. Cardiac stimulants such as adrenergic agents also have high impact on PPI and PDI network mainly by modulating hubs in the controller sub-network. Members of the “Sex hormones and modulators of the genital system” ATC class act on AR.

The “antineoplastic drug” methotrexate mainly acts through the accumulation of adenosine, but the other antineoplastic agents may act in a different manner like the inhibition of keratinocyte hyperproliferation [163]. Studies or case reports already suggest efficacy of some antineoplastic drugs, but several new possible agents were found in our analysis [98,164,165]. Mental stress is known to trigger psoriasis and connection between the neuroendocrine system and skin immune system has already been reported [26,166]. Thus, this is not surprising, that numerous drugs acting on the CNS are enriched in results. A lot of other drugs, which are either classified in ATC classes or just drug candidates, are found. For example kainic acid, cocaine, the HDAC inhibitor sodium butyrate, the PKC inhibitor bisindolylmaleimide I etc. (Table 7)

Our results suggested, that the fusion of different intracellular networks with chemical-protein interaction networks can be an effective method for the detection of potentially effective drugs in the treatment of psoriasis. Our intracellular networks were constructed with the use of DEGs, which characterize the lesional phenotype in itself. The integration of drug-protein interaction data in this system seemed to be a powerful tool for drug discovery of psoriasis. The rather, that other research groups have proven the efficacy of some predicted drugs since the

publication of our results. For example, the role of aryl hydrocarbon receptor in chronic inflammatory skin diseases was reported recently and drugs targeting this receptor were found in our analysis (Table 7) [167].

### ***8.5. The place of systems biology in dermatological research***

Large amount of “omics” data was generated in the past decades in parallel with the improvement of screening technologies. As our VVC study showed, virulence factors can be identified with the use of experimental models and carrying out transcriptome analysis. New and important findings can be acquired by the analysis of published data too. We were able not only to identify new proteins in the pathogenesis of psoriasis, but to find new therapeutic options for the disease.

We have demonstrated two examples, how large scale data of multifactorial dermatological diseases can be used. The use of large datasets, analyzing them with the tools of bioinformatics and biostatistics is inevitable in this modern era of biomedical research. We have become able to understand complex processes, construct models of diseases and treat them more effectively.

## Acknowledgement

Firstly, I would like to express my sincere gratitude to my advisors, Prof. Dr. Lajos Kemény and Dr. Lóránt Lakatos for the continuous support of my PhD study and related research, for their patience, motivation, and immense knowledge.

My sincere thanks also goes to Dr. Éva Kondorosi and Dr. István Nagy, who gave access to the most modern laboratory and research facilities for *C. albicans* studies in Biological Research Centre, Szeged. Without their precious support it would not be possible to conduct this research.

I thank my fellow labmates and colleagues for the stimulating discussions and for all the fun we have had. I am grateful to Dr. Csaba Pál for giving support for my research last year.

Last but not the least, I would like to say thanks to my family and especially to my fiancée, Melinda for supporting me throughout my life in general.

## References

1. Kitano H (2002) Computational systems biology. *Nature* 420: 206-210.
2. Gill SR, Pop M, Deboy RT, Eckburg PB, Turnbaugh PJ, et al. (2006) Metagenomic analysis of the human distal gut microbiome. *Science* 312: 1355-1359.
3. Baddal B, Muzzi A, Censini S, Calogero RA, Torricelli G, et al. (2015) Dual RNA-seq of Nontypeable *Haemophilus influenzae* and Host Cell Transcriptomes Reveals Novel Insights into Host-Pathogen Cross Talk. *MBio* 6.
4. Berg EL (2014) Systems biology in drug discovery and development. *Drug Discov Today* 19: 113-125.
5. Servant N, Gravier E, Gestraud P, Laurent C, Paccard C, et al. (2010) EMA - A R package for Easy Microarray data analysis. *BMC Res Notes* 3: 277.
6. Fidel PL, Jr. (2007) History and update on host defense against vaginal candidiasis. *Am J Reprod Immunol* 57: 2-12.
7. Yapar N (2014) Epidemiology and risk factors for invasive candidiasis. *Ther Clin Risk Manag* 10: 95-105.
8. Al-Hebshi NN, Al-Maswary EA, Al-Hammadi ZO, Ghoname N (2015) Salivary *Candida* species carriage patterns and their relation to caries experience among yemeni children. *Oral Health Prev Dent* 13: 41-49.
9. de Leon EM, Jacober SJ, Sobel JD, Foxman B (2002) Prevalence and risk factors for vaginal *Candida* colonization in women with type 1 and type 2 diabetes. *BMC Infect Dis* 2: 1.
10. Sobel JD (2016) Recurrent vulvovaginal candidiasis. *Am J Obstet Gynecol* 214: 15-21.
11. Sudbery PE (2011) Growth of *Candida albicans* hyphae. *Nat Rev Microbiol* 9: 737-748.
12. Mayer FL, Wilson D, Hube B (2013) *Candida albicans* pathogenicity mechanisms. *Virulence* 4: 119-128.
13. Gow NA, van de Veerdonk FL, Brown AJ, Netea MG (2012) *Candida albicans* morphogenesis and host defence: discriminating invasion from colonization. *Nat Rev Microbiol* 10: 112-122.
14. Finkel JS, Xu W, Huang D, Hill EM, Desai JV, et al. (2012) Portrait of *Candida albicans* adherence regulators. *PLoS Pathog* 8: e1002525.
15. Wu H, Downs D, Ghosh K, Ghosh AK, Staib P, et al. (2013) *Candida albicans* secreted aspartic proteases 4-6 induce apoptosis of epithelial cells by a novel Trojan horse mechanism. *FASEB J* 27: 2132-2144.
16. Netea MG, Brown GD, Kullberg BJ, Gow NA (2008) An integrated model of the recognition of *Candida albicans* by the innate immune system. *Nat Rev Microbiol* 6: 67-78.
17. Pitarch A, Nombela C, Gil C (2014) Serum antibody signature directed against *Candida albicans* Hsp90 and enolase detects invasive candidiasis in non-neutropenic patients. *J Proteome Res* 13: 5165-5184.
18. Naglik JR, Fostira F, Ruprai J, Staab JF, Challacombe SJ, et al. (2006) *Candida albicans* HWP1 gene expression and host antibody responses in colonization and disease. *J Med Microbiol* 55: 1323-1327.
19. Naglik JR, Moyes DL, Wachtler B, Hube B (2011) *Candida albicans* interactions with epithelial cells and mucosal immunity. *Microbes Infect* 13: 963-976.
20. Dustin ML (2014) The immunological synapse. *Cancer Immunol Res* 2: 1023-1033.
21. Gozalbo D, Maneu V, Gil ML (2014) Role of IFN-gamma in immune responses to *Candida albicans* infections. *Front Biosci (Landmark Ed)* 19: 1279-1290.
22. Parisi R, Symmons DP, Griffiths CE, Ashcroft DM (2013) Global epidemiology of psoriasis: a systematic review of incidence and prevalence. *J Invest Dermatol* 133: 377-385.
23. Rachakonda TD, Schupp CW, Armstrong AW (2014) Psoriasis prevalence among adults in the United States. *J Am Acad Dermatol* 70: 512-516.
24. Bologna J, Jorizzo JL, Schaffer JV (2012) *Dermatology*. [Philadelphia]: Elsevier Saunders. 2 v. (xxv, 2572, 2573 p.) p.
25. Tsoi LC, Spain SL, Knight J, Ellinghaus E, Stuart PE, et al. (2012) Identification of 15 new psoriasis susceptibility loci highlights the role of innate immunity. *Nat Genet* 44: 1341-1348.

26. Griffiths CE, Barker JN (2007) Pathogenesis and clinical features of psoriasis. *Lancet* 370: 263-271.
27. Farkas A, Kemeny L (2012) Monocyte-derived interferon-alpha primed dendritic cells in the pathogenesis of psoriasis: new pieces in the puzzle. *Int Immunopharmacol* 13: 215-218.
28. Armstrong AW, Harskamp CT, Armstrong EJ (2013) Psoriasis and metabolic syndrome: A systematic review and meta-analysis of observational studies. *J Am Acad Dermatol*.
29. Smith CH, Jackson K, Bashir SJ, Perez A, Chew AL, et al. (2006) Infliximab for severe, treatment-resistant psoriasis: a prospective, open-label study. *Br J Dermatol* 155: 160-169.
30. Marzancola MG, Sedighi A, Li PC (2016) DNA Microarray-Based Diagnostics. *Methods Mol Biol* 1368: 161-178.
31. Li PC, Sedighi A, Wang L *Microarray Technology*.
32. Campaign A, Yang YH (2010) Comparison study of microarray meta-analysis methods. *BMC Bioinformatics* 11: 408.
33. Ronaghi M, Karamohamed S, Pettersson B, Uhlen M, Nyren P (1996) Real-time DNA sequencing using detection of pyrophosphate release. *Anal Biochem* 242: 84-89.
34. Bahassi el M, Stambrook PJ (2014) Next-generation sequencing technologies: breaking the sound barrier of human genetics. *Mutagenesis* 29: 303-310.
35. Valouev A, Ichikawa J, Tonthat T, Stuart J, Ranade S, et al. (2008) A high-resolution, nucleosome position map of *C. elegans* reveals a lack of universal sequence-dictated positioning. *Genome Res* 18: 1051-1063.
36. Junker BH, Schreiber F (2011) *Analysis of biological networks*: John Wiley & Sons.
37. Barabasi AL, Albert R (1999) Emergence of scaling in random networks. *Science* 286: 509-512.
38. Brandes U, Erlebach T (2005) *Network analysis : methodological foundations*. Berlin ; New York: Springer. xii, 471 p. p.
39. Ingram PJ, Stumpf MP, Stark J (2006) Network motifs: structure does not determine function. *BMC Genomics* 7: 108.
40. Barabasi AL (2009) Scale-free networks: a decade and beyond. *Science* 325: 412-413.
41. Bader GD, Cary MP, Sander C (2006) Pathguide: a pathway resource list. *Nucleic Acids Res* 34: D504-506.
42. Szklarczyk D, Franceschini A, Kuhn M, Simonovic M, Roth A, et al. (2011) The STRING database in 2011: functional interaction networks of proteins, globally integrated and scored. *Nucleic Acids Res* 39: D561-568.
43. Robertson G, Bilenky M, Lin K, He A, Yuen W, et al. (2006) cisRED: a database system for genome-scale computational discovery of regulatory elements. *Nucleic Acids Res* 34: D68-73.
44. Rajan N, Pruden DL, Kaznari H, Cao Q, Anderson BE, et al. (2000) Characterization of an immortalized human vaginal epithelial cell line. *J Urol* 163: 616-622.
45. Pivarcsi A, Nagy I, Koreck A, Kis K, Kenderessy-Szabo A, et al. (2005) Microbial compounds induce the expression of pro-inflammatory cytokines, chemokines and human beta-defensin-2 in vaginal epithelial cells. *Microbes Infect* 7: 1117-1127.
46. Kiss L, Walter FR, Bocsik A, Veszelka S, Ozsvari B, et al. (2013) Kinetic analysis of the toxicity of pharmaceutical excipients Cremophor EL and RH40 on endothelial and epithelial cells. *J Pharm Sci* 102: 1173-1181.
47. Kurti L, Gaspar R, Marki A, Kapolna E, Bocsik A, et al. (2013) In vitro and in vivo characterization of meloxicam nanoparticles designed for nasal administration. *Eur J Pharm Sci* 50: 86-92.
48. Ordogh L, Voros A, Nagy I, Kondorosi E, Kereszt A (2014) Symbiotic plant peptides eliminate *Candida albicans* both in vitro and in an epithelial infection model and inhibit the proliferation of immortalized human cells. *Biomed Res Int* 2014: 320796.
49. Naseem S, Gunasekera A, Araya E, Konopka JB (2011) N-acetylglucosamine (GlcNAc) induction of hyphal morphogenesis and transcriptional responses in *Candida albicans* are not dependent on its metabolism. *J Biol Chem* 286: 28671-28680.
50. Fodor E, Zsigmond A, Horvath B, Molnar J, Nagy I, et al. (2013) Full transcriptome analysis of early dorsoventral patterning in zebrafish. *PLoS One* 8: e70053.

51. van het Hoog M, Rast TJ, Martchenko M, Grindle S, Dignard D, et al. (2007) Assembly of the *Candida albicans* genome into sixteen supercontigs aligned on the eight chromosomes. *Genome Biol* 8: R52.
52. Robinson MD, Oshlack A (2010) A scaling normalization method for differential expression analysis of RNA-seq data. *Genome Biol* 11: R25.
53. Storey JD, Tibshirani R (2003) Statistical significance for genomewide studies. *Proc Natl Acad Sci U S A* 100: 9440-9445.
54. Wang L, Feng Z, Wang X, Wang X, Zhang X (2010) DEGseq: an R package for identifying differentially expressed genes from RNA-seq data. *Bioinformatics* 26: 136-138.
55. Kauffmann A, Gentleman R, Huber W (2009) arrayQualityMetrics--a bioconductor package for quality assessment of microarray data. *Bioinformatics* 25: 415-416.
56. Kang DD, Sibille E, Kaminski N, Tseng GC (2012) MetaQC: objective quality control and inclusion/exclusion criteria for genomic meta-analysis. *Nucleic Acids Res* 40: e15.
57. Subramanian A, Tamayo P, Mootha VK, Mukherjee S, Ebert BL, et al. (2005) Gene set enrichment analysis: a knowledge-based approach for interpreting genome-wide expression profiles. *Proc Natl Acad Sci U S A* 102: 15545-15550.
58. Wang X, Kang DD, Shen K, Song C, Lu S, et al. (2012) An R package suite for microarray meta-analysis in quality control, differentially expressed gene analysis and pathway enrichment detection. *Bioinformatics* 28: 2534-2536.
59. Derkach A, Lawless JF, Sun L (2013) Robust and powerful tests for rare variants using Fisher's method to combine evidence of association from two or more complementary tests. *Genet Epidemiol* 37: 110-121.
60. Morgan AA, Khatri P, Jones RH, Sarwal MM, Butte AJ (2010) Comparison of multiplex meta analysis techniques for understanding the acute rejection of solid organ transplants. *BMC Bioinformatics* 11 Suppl 9: S6.
61. Kuhn M, Szklarczyk D, Franceschini A, von Mering C, Jensen LJ, et al. (2012) STITCH 3: zooming in on protein-chemical interactions. *Nucleic Acids Res* 40: D876-880.
62. Wingender E, Dietze P, Karas H, Knuppel R (1996) TRANSFAC: a database on transcription factors and their DNA binding sites. *Nucleic Acids Res* 24: 238-241.
63. Sandelin A, Alkema W, Engstrom P, Wasserman WW, Lenhard B (2004) JASPAR: an open-access database for eukaryotic transcription factor binding profiles. *Nucleic Acids Res* 32: D91-94.
64. Smoot ME, Ono K, Ruscheinski J, Wang PL, Ideker T (2011) Cytoscape 2.8: new features for data integration and network visualization. *Bioinformatics* 27: 431-432.
65. Newman M (2005) Power laws, Pareto distributions and Zipf's law. *Contemporary Physics* 46: 323-351.
66. Li X, Stones DS, Wang H, Deng H, Liu X, et al. (2012) NetMODE: network motif detection without Nauty. *PLoS One* 7: e50093.
67. Ferro A, Giugno R, Pigola G, Pulvirenti A, Skripin D, et al. (2007) NetMatch: a Cytoscape plugin for searching biological networks. *Bioinformatics* 23: 910-912.
68. Zakikhany K, Naglik JR, Schmidt-Westhausen A, Holland G, Schaller M, et al. (2007) In vivo transcript profiling of *Candida albicans* identifies a gene essential for interepithelial dissemination. *Cell Microbiol* 9: 2938-2954.
69. Kadosh D, Johnson AD (2005) Induction of the *Candida albicans* filamentous growth program by relief of transcriptional repression: a genome-wide analysis. *Mol Biol Cell* 16: 2903-2912.
70. Simonetti N, Strippoli V, Cassone A (1974) Yeast-mycelial conversion induced by N-acetyl-D-glucosamine in *Candida albicans*. *Nature* 250: 344-346.
71. Huang G, Yi S, Sahni N, Daniels KJ, Srikantha T, et al. (2010) N-acetylglucosamine induces white to opaque switching, a mating prerequisite in *Candida albicans*. *PLoS Pathog* 6: e1000806.
72. Rao KH, Ruhela D, Ghosh S, Abdin MZ, Datta A (2014) N-acetylglucosamine kinase, HXK1 contributes to white-opaque morphological transition in *Candida albicans*. *Biochem Biophys Res Commun* 445: 138-144.
73. Hudson DA, Sciascia QL, Sanders RJ, Norris GE, Edwards PJ, et al. (2004) Identification of the dialysable serum inducer of germ-tube formation in *Candida albicans*. *Microbiology* 150: 3041-3049.

74. Maidan MM, Thevelein JM, Van Dijck P (2005) Carbon source induced yeast-to-hypha transition in *Candida albicans* is dependent on the presence of amino acids and on the G-protein-coupled receptor Gpr1. *Biochem Soc Trans* 33: 291-293.
75. Konopka JB (2012) N-acetylglucosamine (GlcNAc) functions in cell signaling. *Scientifica (Cairo)* 2012.
76. Richard ML, Plaine A (2007) Comprehensive analysis of glycosylphosphatidylinositol-anchored proteins in *Candida albicans*. *Eukaryot Cell* 6: 119-133.
77. Lin MH, Shu JC, Lin LP, Chong KY, Cheng YW, et al. (2015) Elucidating the crucial role of poly N-acetylglucosamine from *Staphylococcus aureus* in cellular adhesion and pathogenesis. *PLoS One* 10: e0124216.
78. Gudjonsson JE, Ding J, Li X, Nair RP, Tejasvi T, et al. (2009) Global gene expression analysis reveals evidence for decreased lipid biosynthesis and increased innate immunity in uninvolved psoriatic skin. *J Invest Dermatol* 129: 2795-2804.
79. Yao Y, Richman L, Morehouse C, de los Reyes M, Higgs BW, et al. (2008) Type I interferon: potential therapeutic target for psoriasis? *PLoS One* 3: e2737.
80. Zaba LC, Suarez-Farinas M, Fuentes-Duculan J, Nograles KE, Guttman-Yassky E, et al. (2009) Effective treatment of psoriasis with etanercept is linked to suppression of IL-17 signaling, not immediate response TNF genes. *J Allergy Clin Immunol* 124: 1022-1010 e1021-1395.
81. Suarez-Farinas M, Li K, Fuentes-Duculan J, Hayden K, Brodmerkel C, et al. (2012) Expanding the psoriasis disease profile: interrogation of the skin and serum of patients with moderate-to-severe psoriasis. *J Invest Dermatol* 132: 2552-2564.
82. Reischl J, Schwenke S, Beekman JM, Mrowietz U, Sturzebecher S, et al. (2007) Increased expression of Wnt5a in psoriatic plaques. *J Invest Dermatol* 127: 163-169.
83. Johnson-Huang LM, Pensabene CA, Shah KR, Pierson KC, Kikuchi T, et al. (2012) Post-therapeutic relapse of psoriasis after CD11a blockade is associated with T cells and inflammatory myeloid DCs. *PLoS One* 7: e30308.
84. Lu X, Jain VV, Finn PW, Perkins DL (2007) Hubs in biological interaction networks exhibit low changes in expression in experimental asthma. *Mol Syst Biol* 3: 98.
85. Beutler B (2009) Microbe sensing, positive feedback loops, and the pathogenesis of inflammatory diseases. *Immunol Rev* 227: 248-263.
86. Ma'ayan A, Lipshtat A, Iyengar R, Sontag ED (2008) Proximity of intracellular regulatory networks to monotone systems. *IET Syst Biol* 2: 103-112.
87. Brandman O, Ferrell JE, Jr., Li R, Meyer T (2005) Interlinked fast and slow positive feedback loops drive reliable cell decisions. *Science* 310: 496-498.
88. Miller GC, Britt H (1995) A new drug classification for computer systems: the ATC extension code. *Int J Biomed Comput* 40: 121-124.
89. Kanehisa M, Goto S, Hattori M, Aoki-Kinoshita KF, Itoh M, et al. (2006) From genomics to chemical genomics: new developments in KEGG. *Nucleic Acids Res* 34: D354-357.
90. Menter A, Griffiths CE (2007) Current and future management of psoriasis. *Lancet* 370: 272-284.
91. Brauchli YB, Jick SS, Curtin F, Meier CR (2008) Association between use of thiazolidinediones or other oral antidiabetics and psoriasis: A population based case-control study. *J Am Acad Dermatol* 58: 421-429.
92. Malhotra A, Shafiq N, Rajagopalan S, Dogra S, Malhotra S (2012) Thiazolidinediones for plaque psoriasis: a systematic review and meta-analysis. *Evid Based Med* 17: 171-176.
93. Ellis CN, Varani J, Fisher GJ, Zeigler ME, Pershadsingh HA, et al. (2000) Troglitazone improves psoriasis and normalizes models of proliferative skin disease: ligands for peroxisome proliferator-activated receptor-gamma inhibit keratinocyte proliferation. *Arch Dermatol* 136: 609-616.
94. Shirinsky IV, Shirinsky VS (2007) Efficacy of simvastatin in plaque psoriasis: A pilot study. *J Am Acad Dermatol* 57: 529-531.
95. Faghihi T, Radfar M, Mehrabian Z, Ehsani AH, Rezaei Hemami M (2011) Atorvastatin for the treatment of plaque-type psoriasis. *Pharmacotherapy* 31: 1045-1050.
96. Lebwohl M (1999) The role of salicylic acid in the treatment of psoriasis. *Int J Dermatol* 38: 16-24.

97. de Jong EM, Menke HE, van Praag MC, van De Kerkhof PC (1999) Dystrophic psoriatic fingernails treated with 1% 5-fluorouracil in a nail penetration-enhancing vehicle: a double-blind study. *Dermatology* 199: 313-318.
98. Ehrlich A, Booher S, Becerra Y, Borris DL, Figg WD, et al. (2004) Micellar paclitaxel improves severe psoriasis in a prospective phase II pilot study. *J Am Acad Dermatol* 50: 533-540.
99. Vali A, Asilian A, Khalesi E, Khoddami L, Shahtalebi M, et al. (2005) Evaluation of the efficacy of topical caffeine in the treatment of psoriasis vulgaris. *J Dermatolog Treat* 16: 234-237.
100. Cohen AD, Kagen M, Friger M, Halevy S (2001) Calcium channel blockers intake and psoriasis: a case-control study. *Acta Derm Venereol* 81: 347-349.
101. Papakostantinou E, Xenos K, Markantonis SL, Druska S, Stratigos A, et al. (2005) Efficacy of 2 weeks' application of theophylline ointment in psoriasis vulgaris. *J Dermatolog Treat* 16: 169-170.
102. Gulliver WP, Donsky HJ (2005) A report on three recent clinical trials using Mahonia aquifolium 10% topical cream and a review of the worldwide clinical experience with Mahonia aquifolium for the treatment of plaque psoriasis. *Am J Ther* 12: 398-406.
103. Han R, Rostami-Yazdi M, Gerdes S, Mrowietz U (2012) Triptolide in the treatment of psoriasis and other immune-mediated inflammatory diseases. *Br J Clin Pharmacol* 74: 424-436.
104. Tsankov N, Grozdev I (2011) Rifampicin--a mild immunosuppressive agent for psoriasis. *J Dermatolog Treat* 22: 62-64.
105. Kurd SK, Smith N, VanVoorhees A, Troxel AB, Badmaev V, et al. (2008) Oral curcumin in the treatment of moderate to severe psoriasis vulgaris: A prospective clinical trial. *J Am Acad Dermatol* 58: 625-631.
106. Kippenberger S, Loitsch SM, Grundmann-Kollmann M, Simon S, Dang TA, et al. (2001) Activators of peroxisome proliferator-activated receptors protect human skin from ultraviolet-B-light-induced inflammation. *J Invest Dermatol* 117: 1430-1436.
107. Kim TG, Byamba D, Wu WH, Lee MG (2011) Statins inhibit chemotactic interaction between CCL20 and CCR6 in vitro: possible relevance to psoriasis treatment. *Exp Dermatol* 20: 855-857.
108. Sticozzi C, Belmonte G, Cervellati F, Di Capua A, Maioli E, et al. (2013) Antiproliferative effect of two novel COX-2 inhibitors on human keratinocytes. *Eur J Pharm Sci* 49: 133-141.
109. Young CN, Koepke JI, Terlecky LJ, Borkin MS, Boyd Savoy L, et al. (2008) Reactive oxygen species in tumor necrosis factor-alpha-activated primary human keratinocytes: implications for psoriasis and inflammatory skin disease. *J Invest Dermatol* 128: 2606-2614.
110. Soler DC, McCormick TS (2011) The dark side of regulatory T cells in psoriasis. *J Invest Dermatol* 131: 1785-1786.
111. Tse WP, Cheng CH, Che CT, Lin ZX (2008) Arsenic trioxide, arsenic pentoxide, and arsenic iodide inhibit human keratinocyte proliferation through the induction of apoptosis. *J Pharmacol Exp Ther* 326: 388-394.
112. Santamaria LF, Torres R, Gimenez-Arnau AM, Gimenez-Camarasa JM, Ryder H, et al. (1999) Rolipram inhibits staphylococcal enterotoxin B-mediated induction of the human skin-homing receptor on T lymphocytes. *J Invest Dermatol* 113: 82-86.
113. Maioli E, Valacchi G (2010) Rottlerin: bases for a possible usage in psoriasis. *Curr Drug Metab* 11: 425-430.
114. Ikai K (1995) Exacerbation and induction of psoriasis by angiotensin-converting enzyme inhibitors. *J Am Acad Dermatol* 32: 819.
115. Lamba G, Palaniswamy C, Singh T, Shah D, Lal S, et al. (2011) Psoriasis induced by losartan therapy: a case report and review of the literature. *Am J Ther* 18: e78-80.
116. Woo SM, Huh CH, Park KC, Youn SW (2007) Exacerbation of psoriasis in a chronic myelogenous leukemia patient treated with imatinib. *J Dermatol* 34: 724-726.
117. Sendagorta E, Allegue F, Rocamora A, Ledo A (1987) Generalized pustular psoriasis precipitated by diclofenac and indomethacin. *Dermatologica* 175: 300-301.
118. Latini A, Carducci M (2003) Psoriasis during therapy with olanzapine. *Eur J Dermatol* 13: 404-405.
119. Tan Pei Lin L, Kwek SK (2010) Onset of psoriasis during therapy with fluoxetine. *Gen Hosp Psychiatry* 32: 446 e449-446 e410.



120. Schopf RE, Ockenfels HM, Schultewolter T, Morsches B (1993) Chloroquine stimulates the mitogen-driven lymphocyte proliferation in patients with psoriasis. *Dermatology* 187: 100-103.
121. Chiricozzi A, Saraceno R, Cannizzaro MV, Nistico SP, Chimenti S, et al. (2012) Complete resolution of erythrodermic psoriasis in an HIV and HCV patient unresponsive to antipsoriatic treatments after highly active antiretroviral therapy (Ritonavir, Atazanavir, Emtricitabine, Tenofovir). *Dermatology* 225: 333-337.
122. Pisano C, Tambaro R, Di Maio M, Formato R, Iaffaioli VR, et al. (2004) Complete resolution of psoriasis in a patient treated with stealth liposomal doxorubicin and carboplatin for ovarian cancer. *Arch Dermatol Res* 296: 141-142.
123. Paslin D (1990) Psoriasis without neutrophils. *Int J Dermatol* 29: 37-40.
124. Cagianò R, Bera I, Vermesan D, Flace P, Sabatini R, et al. (2008) Psoriasis disappearance after the first phase of an oncologic treatment: a serendipity case report. *Clin Ter* 159: 421-425.
125. Halverstam CP, Lebwohl M (2008) Nonstandard and off-label therapies for psoriasis. *Clin Dermatol* 26: 546-553.
126. Perlman HH (1972) Remission of psoriasis vulgaris from the use of nerve-blocking agents. *Arch Dermatol* 105: 128-129.
127. Staples J, Klein D (2012) Can nicotine use alleviate symptoms of psoriasis? *Can Fam Physician* 58: 404-408.
128. Zorzou MP, Stratigos A, Efstathiou E, Bamias A (2004) Exacerbation of psoriasis after treatment with an EGFR tyrosine kinase inhibitor. *Acta Derm Venereol* 84: 308-309.
129. Tomás MSJ, Nader-Macías ME (2007) Effect of a medium simulating vaginal fluid on the growth and expression of beneficial characteristics of potentially probiotic lactobacilli. *Communicating Current Research and Educational Topics and Trends in Applied Microbiology* 2: 732-739.
130. Wagner RD, Johnson SJ, Tucker DR (2012) Protection of vaginal epithelial cells with probiotic Lactobacilli and the effect of estrogen against infection by *Candida albicans*.
131. Nadeem SG, Shafiq A, Hakim ST, Anjum Y, Kazm SU (2013) Effect of growth media, pH and temperature on yeast to hyphal transition in *Candida albicans*. *Open Journal of Medical Microbiology* 2013.
132. Ehrström S, Yu A, Rylander E (2006) Glucose in vaginal secretions before and after oral glucose tolerance testing in women with and without recurrent vulvovaginal candidiasis. *Obstetrics & Gynecology* 108: 1432-1437.
133. Lorenz MC, Bender JA, Fink GR (2004) Transcriptional response of *Candida albicans* upon internalization by macrophages. *Eukaryot Cell* 3: 1076-1087.
134. Liebner DA, Huang K, Parvin JD (2014) MMAD: microarray microdissection with analysis of differences is a computational tool for deconvoluting cell type-specific contributions from tissue samples. *Bioinformatics* 30: 682-689.
135. Saliba AE, Westermann AJ, Gorski SA, Vogel J (2014) Single-cell RNA-seq: advances and future challenges. *Nucleic Acids Res* 42: 8845-8860.
136. Kim MK, Park HS, Kim CH, Park HM, Choi W (2002) Inhibitory effect of nikkomycin Z on chitin synthases in *Candida albicans*. *Yeast* 19: 341-349.
137. Romanowska M, al Yacoub N, Seidel H, Donandt S, Gerken H, et al. (2008) PPARdelta enhances keratinocyte proliferation in psoriasis and induces heparin-binding EGF-like growth factor. *J Invest Dermatol* 128: 110-124.
138. Buerger C, Malisiewicz B, Eiser A, Hardt K, Boehncke WH (2013) mTOR and its downstream signalling components are activated in psoriatic skin. *Br J Dermatol*.
139. Goldminz AM, Au SC, Kim N, Gottlieb AB, Lizzul PF (2013) NF-kappaB: An essential transcription factor in psoriasis. *J Dermatol Sci* 69: 89-94.
140. Hampton PJ, Jans R, Flockhart RJ, Parker G, Reynolds NJ (2012) Lithium regulates keratinocyte proliferation via glycogen synthase kinase 3 and NFAT2 (nuclear factor of activated T cells 2). *J Cell Physiol* 227: 1529-1537.
141. Arsic N, Bendris N, Peter M, Begon-Pescia C, Rebouissou C, et al. (2012) A novel function for Cyclin A2: control of cell invasion via RhoA signaling. *J Cell Biol* 196: 147-162.

142. Choi JH, Choi DK, Sohn KC, Kwak SS, Suk J, et al. (2012) Absence of a human DnaJ protein hTid-1S correlates with aberrant actin cytoskeleton organization in lesional psoriatic skin. *J Biol Chem* 287: 25954-25963.
143. Kim WT, Kim H, Katanaev VL, Joon Lee S, Ishitani T, et al. (2012) Dual functions of DP1 promote biphasic Wnt-on and Wnt-off states during anteroposterior neural patterning. *EMBO J* 31: 3384-3397.
144. Johansen C, Funding AT, Otkjaer K, Kragballe K, Jensen UB, et al. (2006) Protein expression of TNF-alpha in psoriatic skin is regulated at a posttranscriptional level by MAPK-activated protein kinase 2. *J Immunol* 176: 1431-1438.
145. Buerger C, Richter B, Woth K, Salgo R, Malisiewicz B, et al. (2012) Interleukin-1beta interferes with epidermal homeostasis through induction of insulin resistance: implications for psoriasis pathogenesis. *J Invest Dermatol* 132: 2206-2214.
146. Jordan CT, Cao L, Roberson ED, Pierson KC, Yang CF, et al. (2012) PSORS2 is due to mutations in CARD14. *Am J Hum Genet* 90: 784-795.
147. Kallimanis PG, Xenos K, Markantonis SL, Stavropoulos P, Margaroni G, et al. (2009) Serum levels of transforming growth factor-beta1 in patients with mild psoriasis vulgaris and effect of treatment with biological drugs. *Clin Exp Dermatol* 34: 582-586.
148. Madonna S, Scarponi C, Sestito R, Pallotta S, Cavani A, et al. (2010) The IFN-gamma-dependent suppressor of cytokine signaling 1 promoter activity is positively regulated by IFN regulatory factor-1 and Sp1 but repressed by growth factor independence-1b and Kruppel-like factor-4, and it is dysregulated in psoriatic keratinocytes. *J Immunol* 185: 2467-2481.
149. Hald A, Andres RM, Salskov-Iversen ML, Kjellerup RB, Iversen L, et al. (2013) STAT1 expression and activation is increased in lesional psoriatic skin. *Br J Dermatol* 168: 302-310.
150. Miyoshi K, Takaishi M, Nakajima K, Ikeda M, Kanda T, et al. (2011) Stat3 as a therapeutic target for the treatment of psoriasis: a clinical feasibility study with STA-21, a Stat3 inhibitor. *J Invest Dermatol* 131: 108-117.
151. Jackson M, Howie SE, Weller R, Sabin E, Hunter JA, et al. (1999) Psoriatic keratinocytes show reduced IRF-1 and STAT-1alpha activation in response to gamma-IFN. *FASEB J* 13: 495-502.
152. Lee TW, Kwon H, Zong H, Yamada E, Vatish M, et al. (2013) Fyn Deficiency Promotes a Preferential Increase in Subcutaneous Adipose Tissue Mass and Decreased Visceral Adipose Tissue Inflammation. *Diabetes*.
153. Smyth D, Phan V, Wang A, McKay DM (2011) Interferon-gamma-induced increases in intestinal epithelial macromolecular permeability requires the Src kinase Fyn. *Lab Invest* 91: 764-777.
154. Hwang MK, Kang NJ, Heo YS, Lee KW, Lee HJ (2009) Fyn kinase is a direct molecular target of delphinidin for the inhibition of cyclooxygenase-2 expression induced by tumor necrosis factor-alpha. *Biochem Pharmacol* 77: 1213-1222.
155. Giustizieri ML, Mascia F, Frezzolini A, De Pita O, Chinni LM, et al. (2001) Keratinocytes from patients with atopic dermatitis and psoriasis show a distinct chemokine production profile in response to T cell-derived cytokines. *J Allergy Clin Immunol* 107: 871-877.
156. Davidovici BB, Sattar N, Prinz J, Puig L, Emery P, et al. (2010) Psoriasis and systemic inflammatory diseases: potential mechanistic links between skin disease and co-morbid conditions. *J Invest Dermatol* 130: 1785-1796.
157. Senturk N, Aydin F, Birinci A, Yuksel EP, Kara N, et al. (2008) Investigation for the leptin 1 and LEP G2548A gene polymorphism in psoriasis. *Eur J Dermatol* 18: 343-344.
158. Michalik L, Wahli W (2007) Peroxisome proliferator-activated receptors (PPARs) in skin health, repair and disease. *Biochim Biophys Acta* 1771: 991-998.
159. Kwon YW, Jang ER, Lee YM, Kim YS, Kwon KS, et al. (2000) Insulin-like growth factor II induces interleukin-6 expression via NFkappaB activation in psoriasis. *Biochem Biophys Res Commun* 278: 312-317.
160. McCurdy CE, Schenk S, Holliday MJ, Philp A, Houck JA, et al. (2012) Attenuated Pik3r1 expression prevents insulin resistance and adipose tissue macrophage accumulation in diet-induced obese mice. *Diabetes* 61: 2495-2505.
161. Lin HY, Yu IC, Wang RS, Chen YT, Liu NC, et al. (2008) Increased hepatic steatosis and insulin resistance in mice lacking hepatic androgen receptor. *Hepatology* 47: 1924-1935.

162. Schwarz W, Schell H, Hornstein OP (1981) Testosterone serum levels in male psoriatics. *Arch Dermatol Res* 270: 377-379.
163. Johnston A, Gudjonsson JE, Sigmundsdottir H, Ludviksson BR, Valdimarsson H (2005) The anti-inflammatory action of methotrexate is not mediated by lymphocyte apoptosis, but by the suppression of activation and adhesion molecules. *Clin Immunol* 114: 154-163.
164. Wang TS, Tsai TF (2012) Intralesional therapy for psoriasis. *J Dermatolog Treat.*
165. Kohn D, Flatau E, Daher O, Zuckerman F (1980) Treatment of psoriasis with daunorubicin and cytarabine. *Arch Dermatol* 116: 1101-1102.
166. Scholzen T, Armstrong CA, Bunnett NW, Luger TA, Olerud JE, et al. (1998) Neuropeptides in the skin: interactions between the neuroendocrine and the skin immune systems. *Exp Dermatol* 7: 81-96.
167. Di Meglio P, Duarte JH, Ahlfors H, Owens ND, Li Y, et al. (2014) Activation of the aryl hydrocarbon receptor dampens the severity of inflammatory skin conditions. *Immunity* 40: 989-1001.

**I.**

**II.**